New model for pyrenoid structure, biogenesis and regulation in different conditions

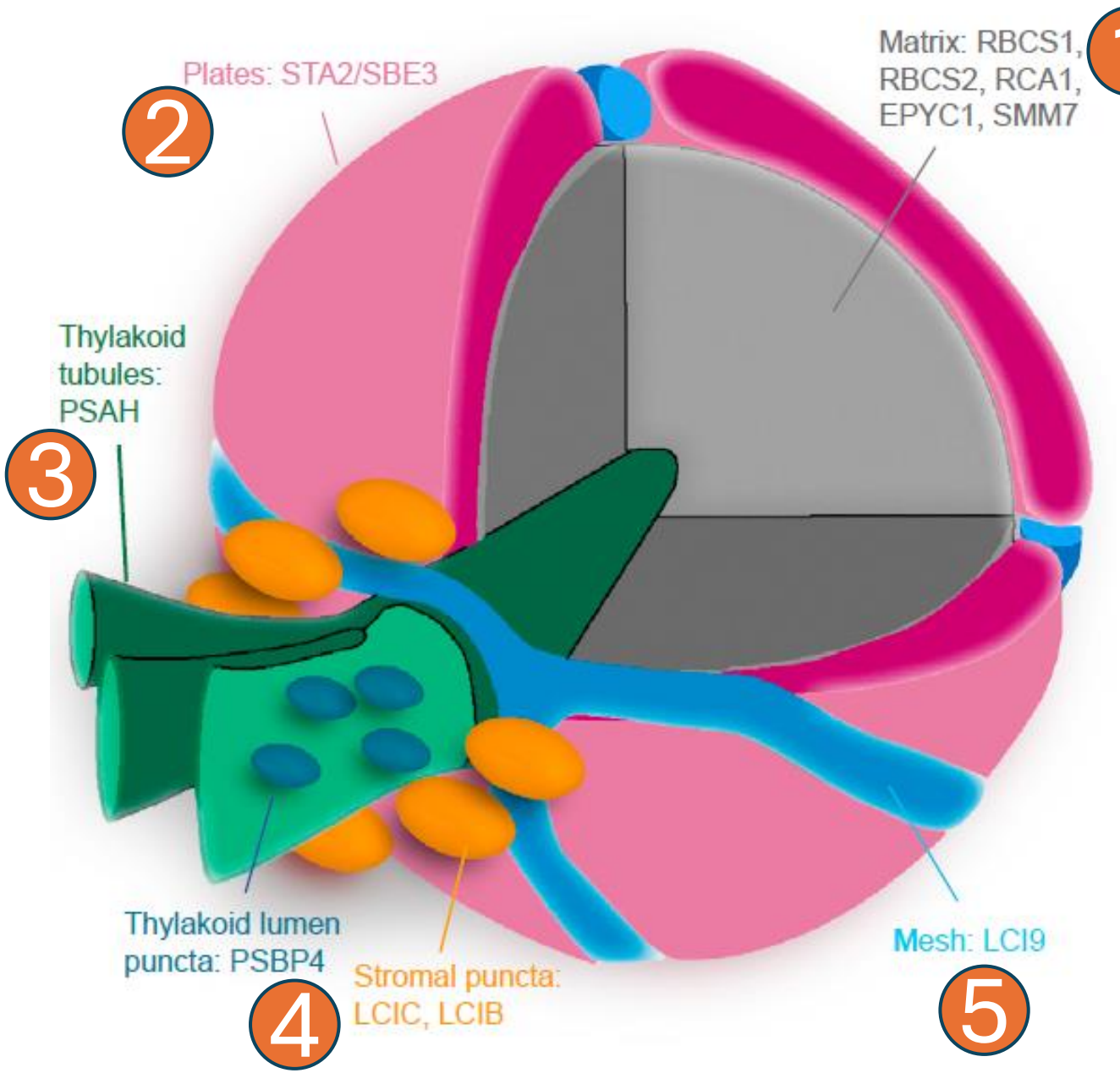

A Putative Methyltransferase Localizes to the Pyrenoid Matrix, role in biogenesis

Cell

Resource

A chloroplast protein atlas reveals punctate structures and spatial organization of biosynthetic pathways

Graphical abstract

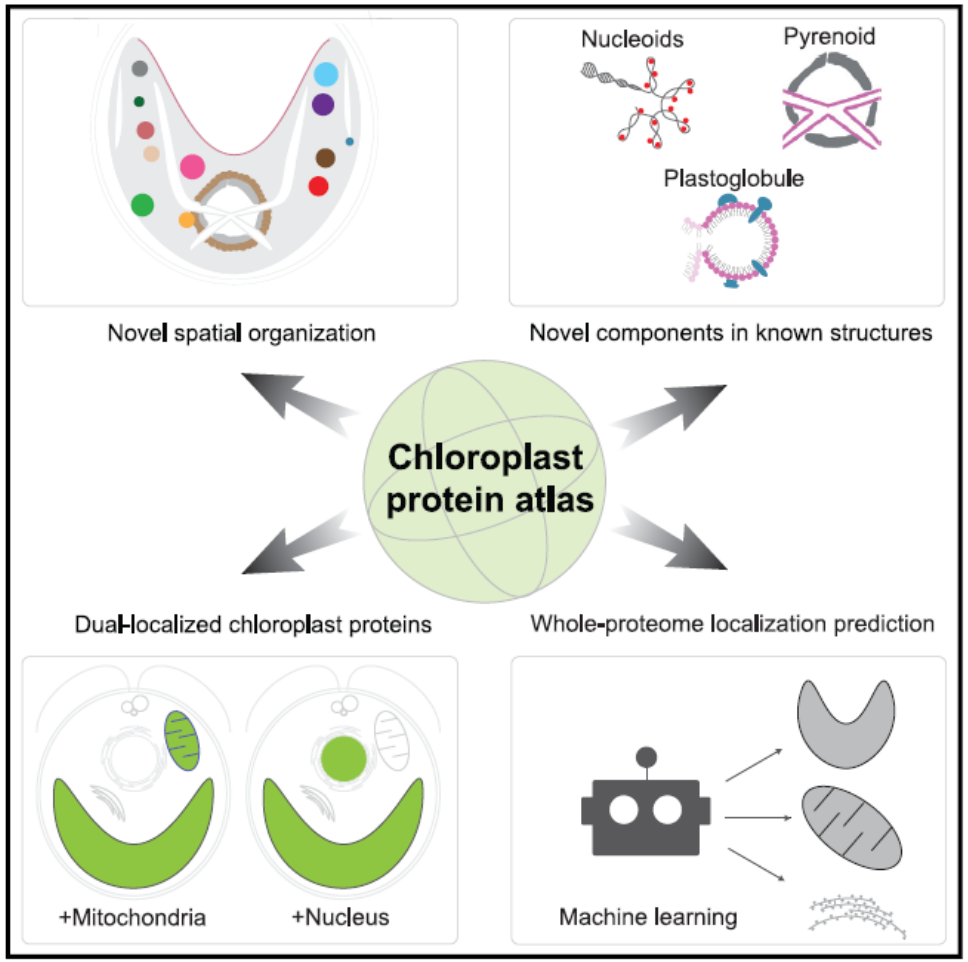

Authors

Lianyong Wang, Weronika Patena, Kelly A. Van Baalen, ..., Danny J. Schnell, Claire D. McWhite, Martin C. Jonikas

Correspondence

mjonikas@princeton.edu

In brief

Localization analyses of 1,034 candidate chloroplast proteins reveal insights into chloroplast architecture and functions in *Chlamydomonas reinhardtii*.

Highlights

- 1,034 candidate chloroplast proteins localized by fluorescent tagging
- This protein atlas reveals chloroplast structures, functional regions, and components
- Dual-organelle localizations suggest extensive cross-compartment coordination
- Atlas-trained machine learning predicts localizations of all *C. reinhardtii* proteins

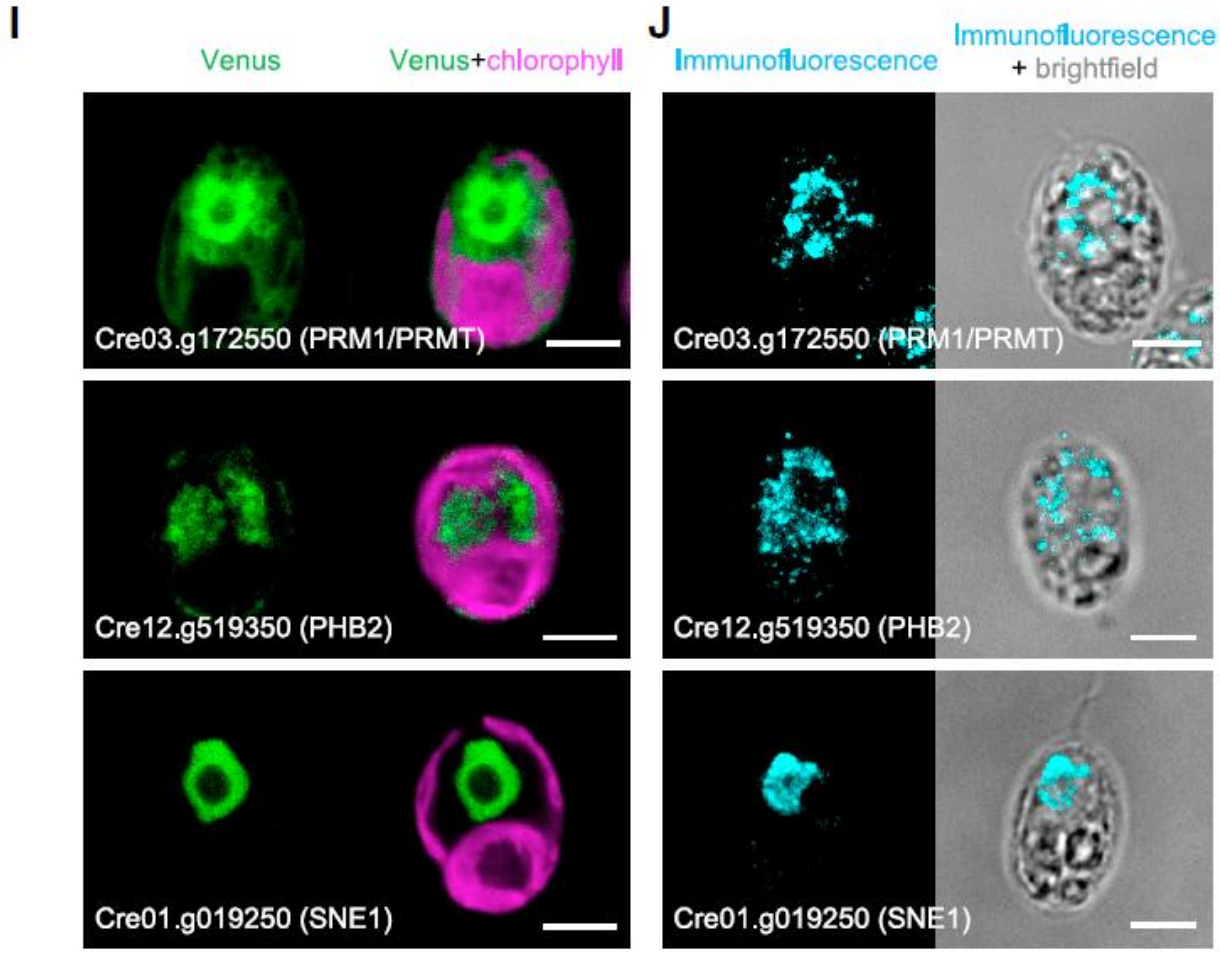

- Localizations of proteins that disagree with proteomics-based localizations in Chlamydomonas: PRM1/PRMT, previously found in chloroplast; PHB2, previously found in mitochondria; SNE1, previously found in flagella

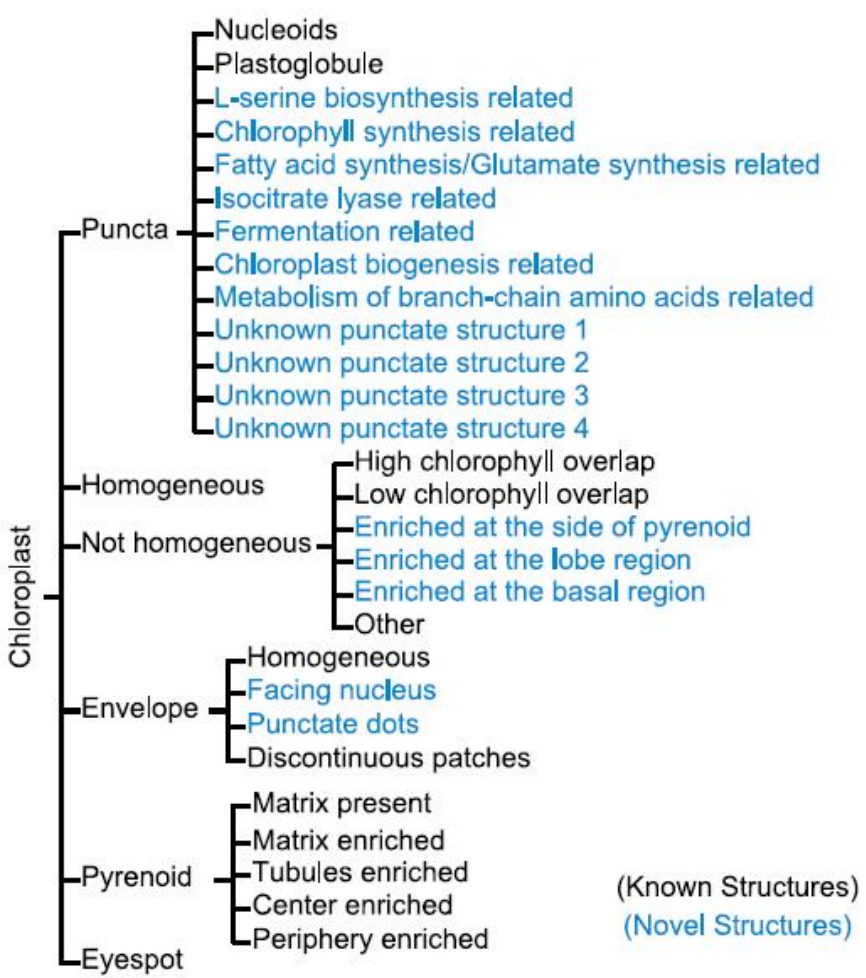

- Decision tree for assigning chloroplast proteins to specific subcellular locations.

FLAG

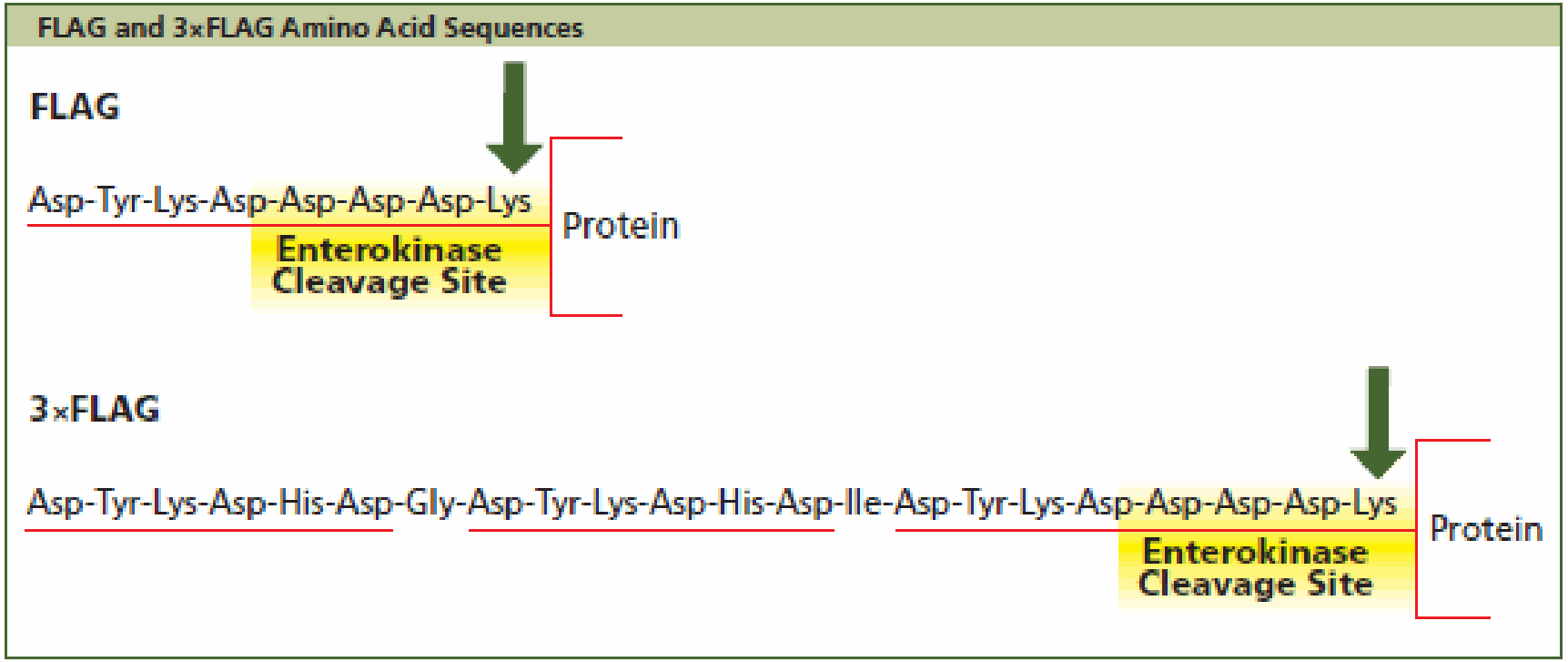
FLAG and 3×FLAG Amino Acid Sequences
FLAG
Asp-Tyr-Lys-Asp-Asp-Asp-Asp-Lys
Enterokinase Cleavage Site
Protein
3×FLAG
Asp-Tyr-Lys-Asp-His-Asp-Gly-Asp-Tyr-Lys-Asp-His-Asp-Ile-Asp-Tyr-Lys-Asp-Asp-Asp-Asp-Lys
Enterokinase Cleavage Site
Protein

Large-scale affinity purification mass spectrometry (AP-MS) approach

- 38 candidates
- 2 different labeling protocols
- Co-localization criteria

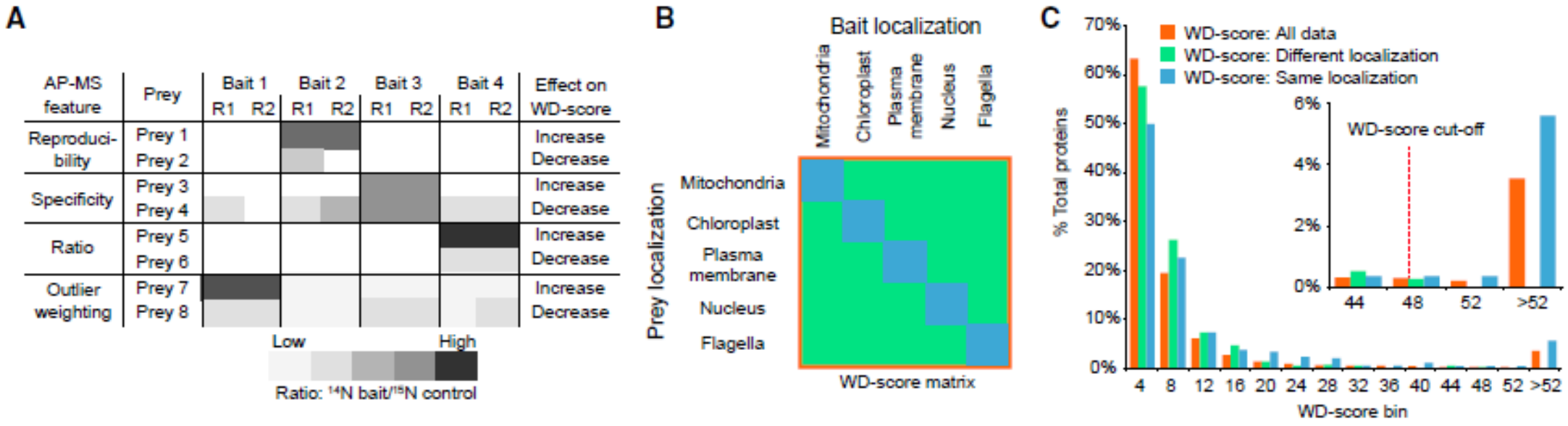

Interesting localization of proteins of photosystem I, photosystem II, CAS and STT7 that are proteins involved in the regulation of photosynthesis activity

Large-scale affinity purification mass spectrometry (AP-MS) approach

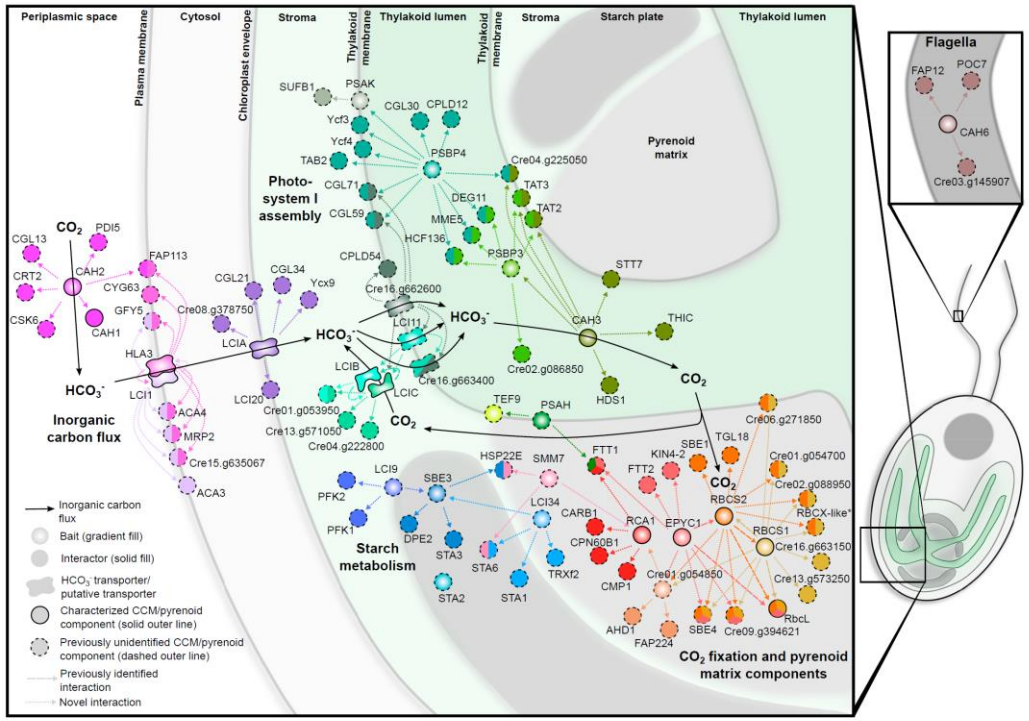

Pyrenoid core
*Cre16.g655050|RBCX-like, Cre06.g273050|CGLD10, Cre09.g386200|OPR36, + 5 more HCIPs
Cre10.g429100, Cre03.g213313
Cre10.g452250
Cre09.g416850
Cre03.g156750|CCT5, Cre03.g168450|CCT8, Cre05.g232750|CNK4, + 16 more HCIPs

Thylakoids
Cre11.g467778, Cre16.g692901
Cre06.g266900, Cre02.g142146
Cre16.g684750
Cre01.g014000
Cre12.g524500|RMT2, Cre07.g328200|PSBP6, Cre11.g475850|ZNJ1, + 6 more HCIPs
Cre17.g729800|ALB3.2, Cre01.g056696, Cre03.g176833
Cre07.g339750|FeC, Cre19.g750547|NDA2, Cre02.g111450|TEF4, + 8 more HCIPs

Chloroplast envelope
Cre05.g230850, 28269781|Ycf78, Cre13.g587100|PCYA1, + 34 more HCIPs

Plasma membrane
Cre08.g360600|ERM4, Cre14.g613950|ABC2, Cre16.g657350, Cre17.g700750|GFY3, + 25 more HCIPs

Extracellular
Cre03.g144564|MMP13, Cre02.g093750|NRX2, Cre09.g393700|MMP3, + 21 more HCIPs

Important to look closer in this interactome.

For example a missing step was the transfer of inorganic carbon from the external environment to the pyrenoid.

They identified 3 proteins that might be involved in bicarbonate transport.

The cellular organelle in algae responsible for one-third of global CO2 fixation

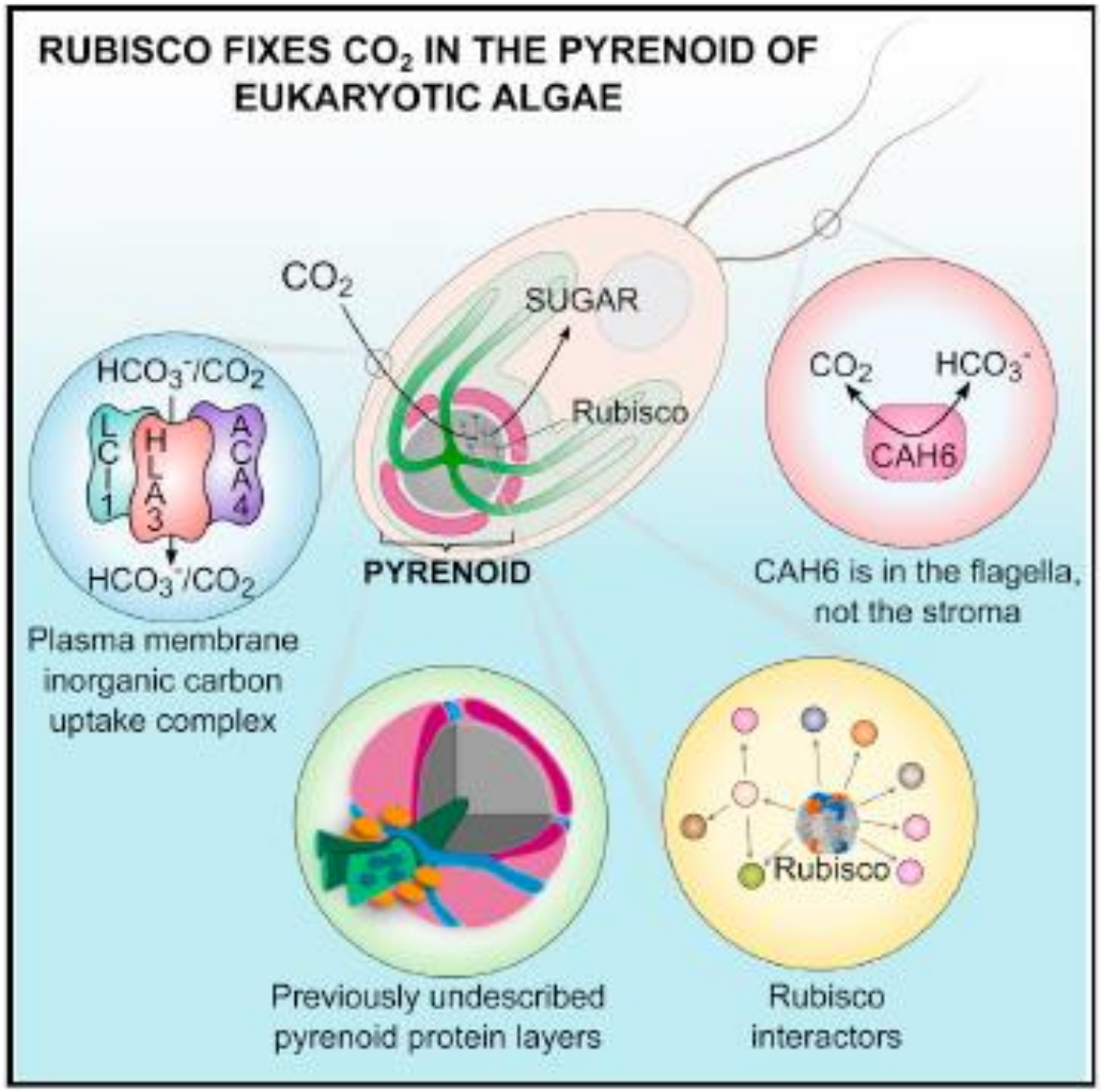

- Localizations and physical interactions of candidate CO2-concentrating mechanism (CCM) proteins were determined
- The data reveal three previously undescribed pyrenoid layers and 89 pyrenoid proteins
- Plasma membrane inorganic carbon transporters LCI1 and HLA3 form a complex
- Carbonic anhydrase 6 localizes to the flagella, changing the model of the CCM

One potential approach for improving yields is the transfer of a CCM into higher plants to increase CO2-fixation rates

EPYC1, a novel protein correlated with RUBISCO activity

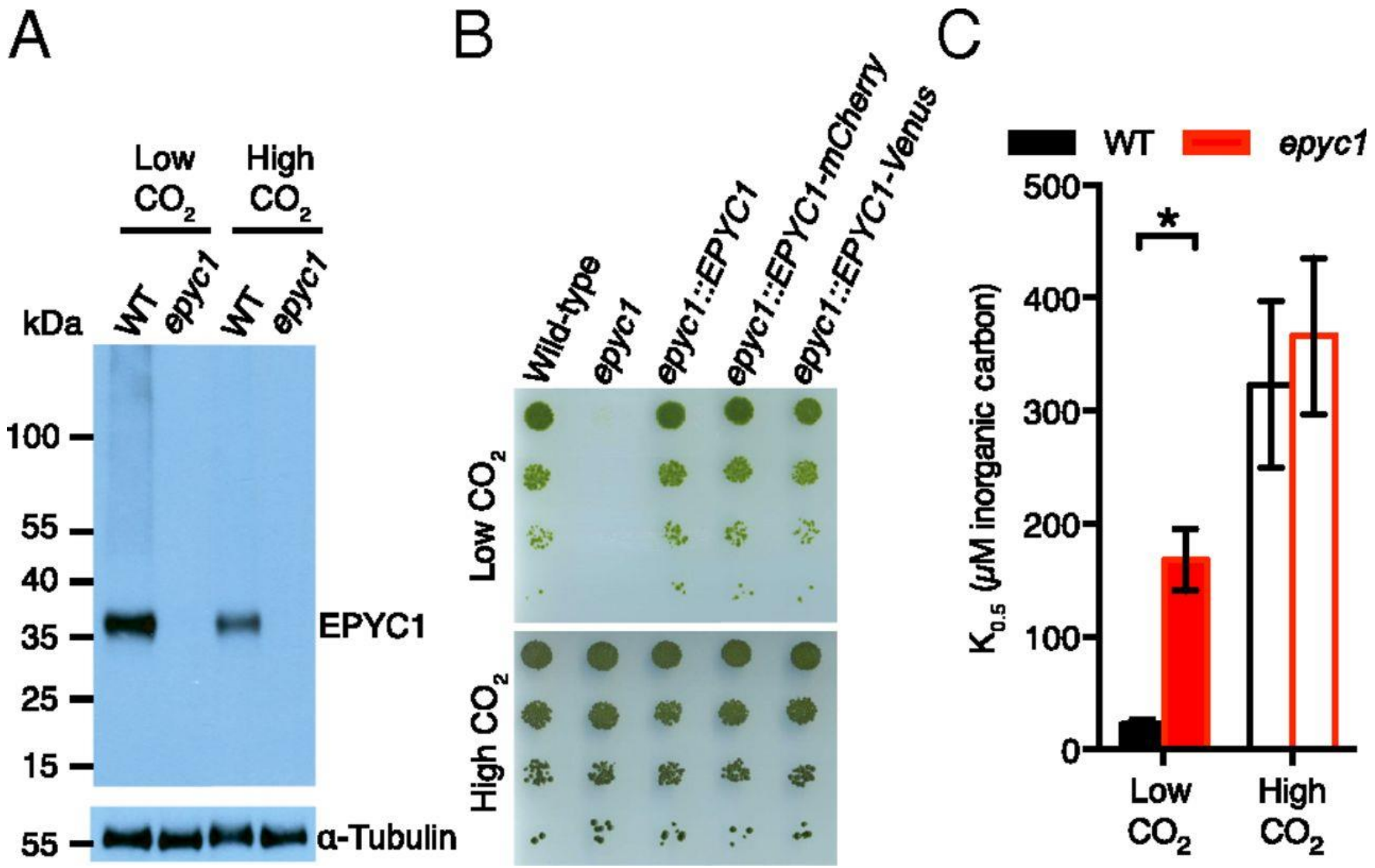

Co-immunopurification

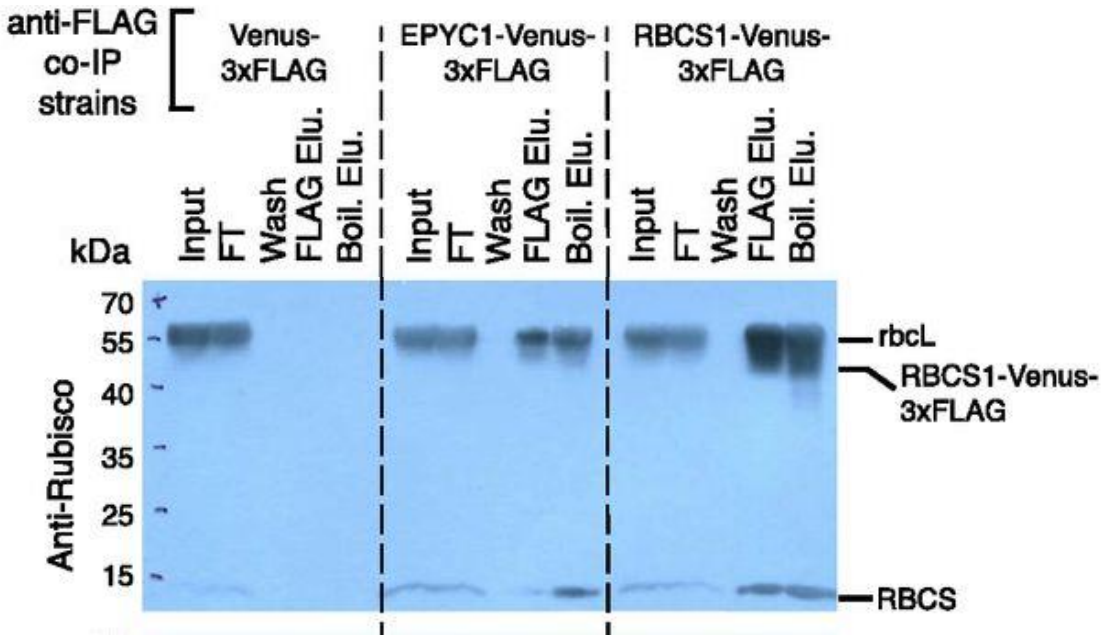

Mathematical models

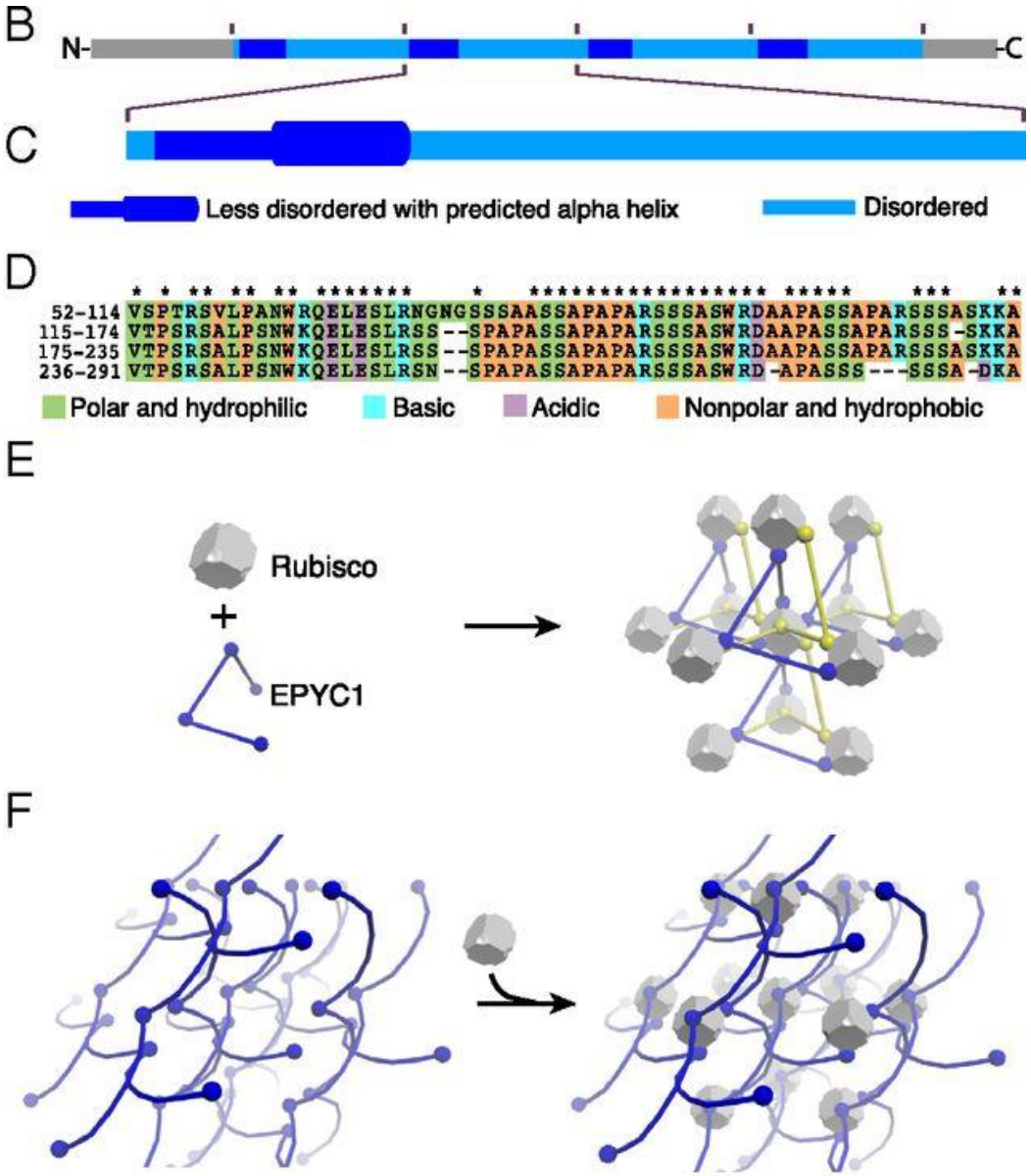

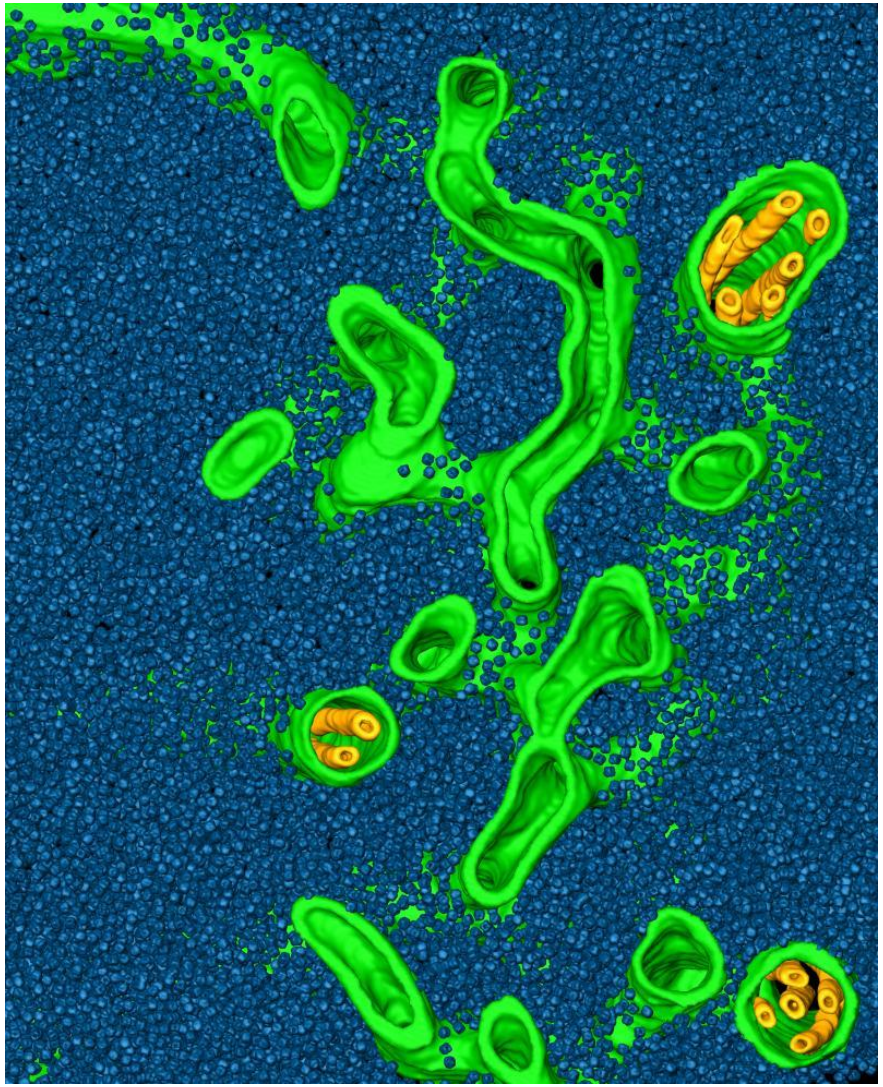

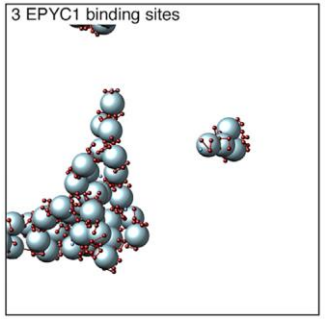
3 EPYC1 binding sites

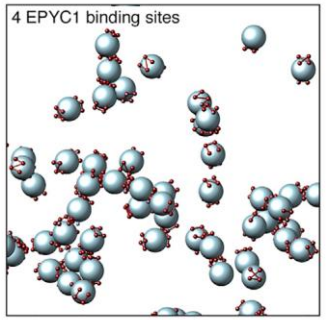
4 EPYC1 binding sites

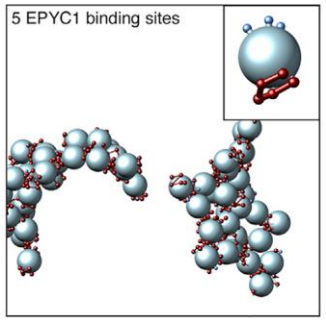
5 EPYC1 binding sites

Cell

Article

The Eukaryotic CO_2-Concentrating Organelle Is Liquid-like and Exhibits Dynamic Reorganization

Elizabeth S. Freeman Rosenzweig,[1,2] Bin Xu,[3,11] Luis Kuhn Cuellar,[4,11] Antonio Martinez-Sanchez,[4] Miroslava Schaffer,[4] Mike Strauss,[5] Heather N. Cartwright,[2] Pierre Ronceray,[6] Jürgen M. Plitzko,[4] Friedrich Förster,[4,9] Ned S. Wingreen,[7,8,*] Benjamin D. Engel,[4,*] Luke C.M. Mackinder,[2,10,12] and Martin C. Jonikas[1,2,8,11,12,13,*]

The Pyrenoid Exhibits Both Fission and *De Novo* Assembly

To enable the first observations of pyrenoid matrix dynamics in living cells, we expressed pyrenoid **matrix proteins tagged with the fluorescent protein Venus** and **imaged them in 3D with fluorescence time-lapse microscopy** during photoautotrophic growth.

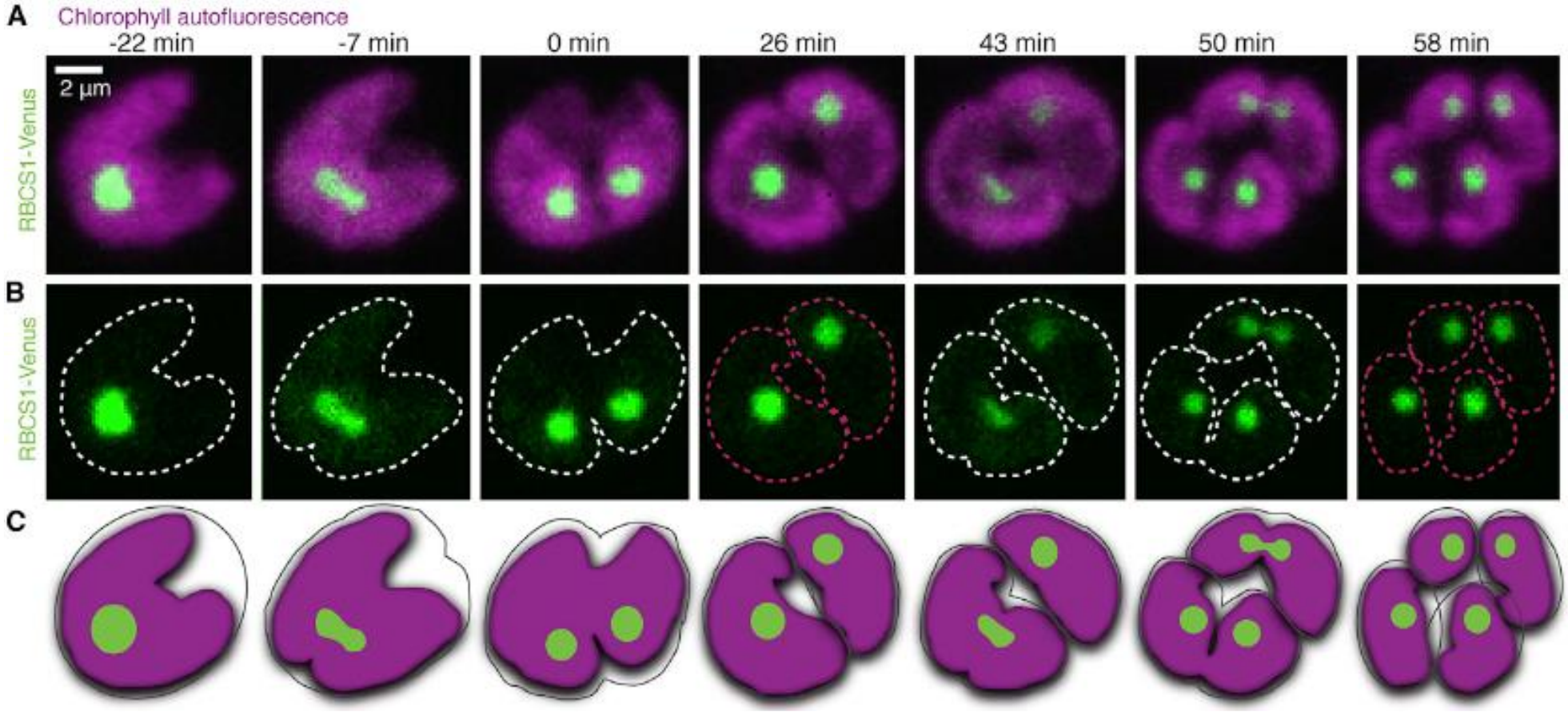

tracked inheritance of the pyrenoid matrix by monitoring Venus-tagged Rubisco small subunit 1 (**RBCS1**) or Venus-tagged **EPYC1** and recorded chlorophyll autofluorescence to follow cellular orientation and chloroplast division

Elongation and then fission

Pyrenoid recall liquid materials with a bridge between two daughter pyrenoids

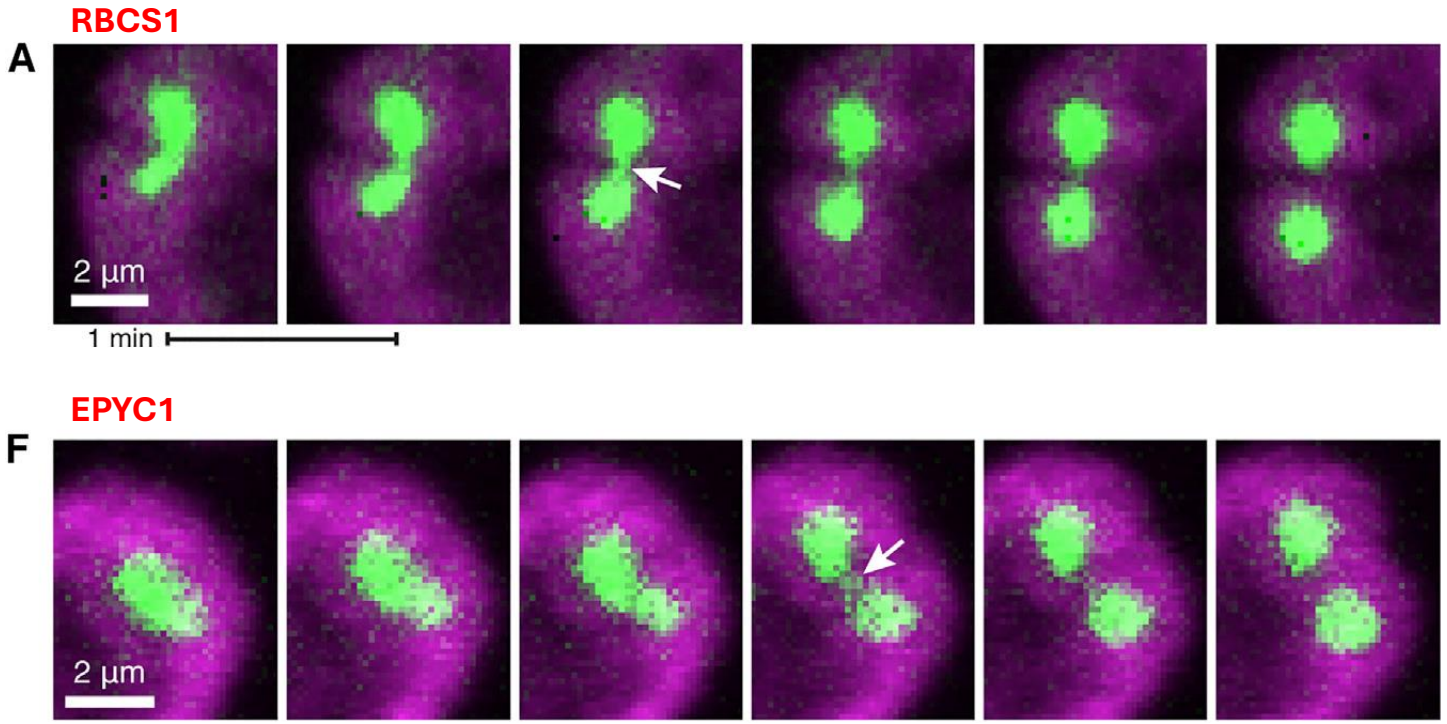

Need for better esolution…

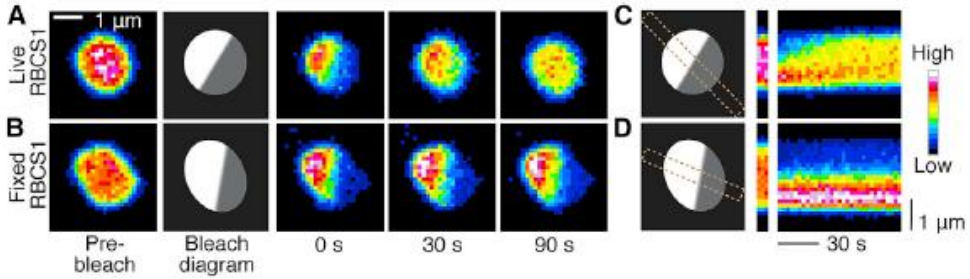

ARTICLES
https://doi.org/10.1038/s41477-020-00811-y
nature plants
Check for updates

The structural basis of Rubisco phase separation in the pyrenoid

Shan He[1], Hui-Ting Chou[2,3], Doreen Matthies[2], Tobias Wunder[4], Moritz T. Meyer[1], Nicky Atkinson[5], Antonio Martinez-Sanchez[6,7], Philip D. Jeffrey[1], Sarah A. Port[1], Weronika Patena[1], Guanhua He[1], Vivian K. Chen[8], Frederick M. Hughson[1], Alistair J. McCormick[5], Oliver Mueller-Cajar[4], Benjamin D. Engel[6,9,10], Zhiheng Yu[2] and Martin C. Jonikas[1]✉

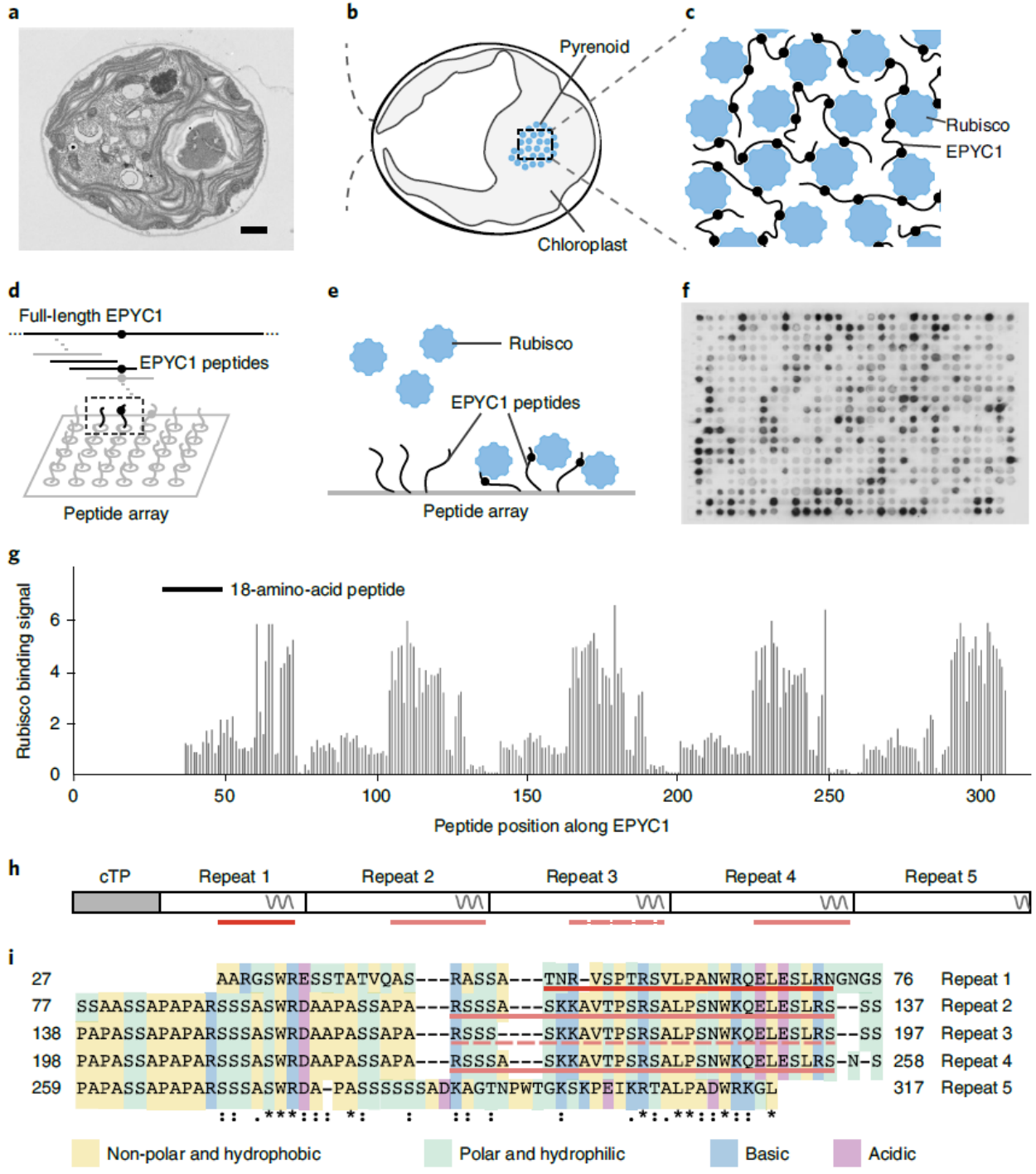

Fig. 1 | EPYC1 consists of five tandem sequence repeats, each of which contains a Rubisco-binding region. a, A representative ($n=15$) transmission electron microscopy (TEM) image of a *C. reinhardtii* cell. Scale bar, 1 µm. **b**, Cartoon depicting the chloroplast and pyrenoid in the image shown in **a**. The blue dots indicate the locations of Rubisco enzymes clustered in the pyrenoid matrix. **c**, We hypothesized that pyrenoid matrix formation is mediated by multivalent interactions between Rubisco and the intrinsically disordered protein EPYC1. **d**, We designed an array of 18 amino acid peptides tiling across the full-length EPYC1 sequence. **e**, Incubation of the array with purified Rubisco allows the identification of peptides that bind to Rubisco. **f**, Image of the Rubisco binding signal from the peptide tiling array. **g**, The Rubisco binding signal was quantified and plotted for each peptide as a function of the position of the middle of the peptide along the EPYC1 sequence. The initial 26 amino acids of EPYC1 correspond to a chloroplast targeting peptide (cTP), which is not present in the mature protein[12]. The results are representative of three independent experiments. **h**, The positions of EPYC1's five sequence repeats are shown to scale with **g**. The predicted α-helical regions are shown as wavy lines. **i**, Primary sequence of EPYC1, with the five sequence repeats aligned. In **h** and **i**, the regions represented by peptides subsequently used for the structural studies are underlined in red ($EPYC1_{49-72}$) and pink ($EPYC1_{106-135}$). $EPYC1_{106-135}$ is an exact match to the underlined sequence of Repeats 2 and 4, and it has a one-amino-acid-difference from the corresponding region in Repeat 3 (dashed underline).

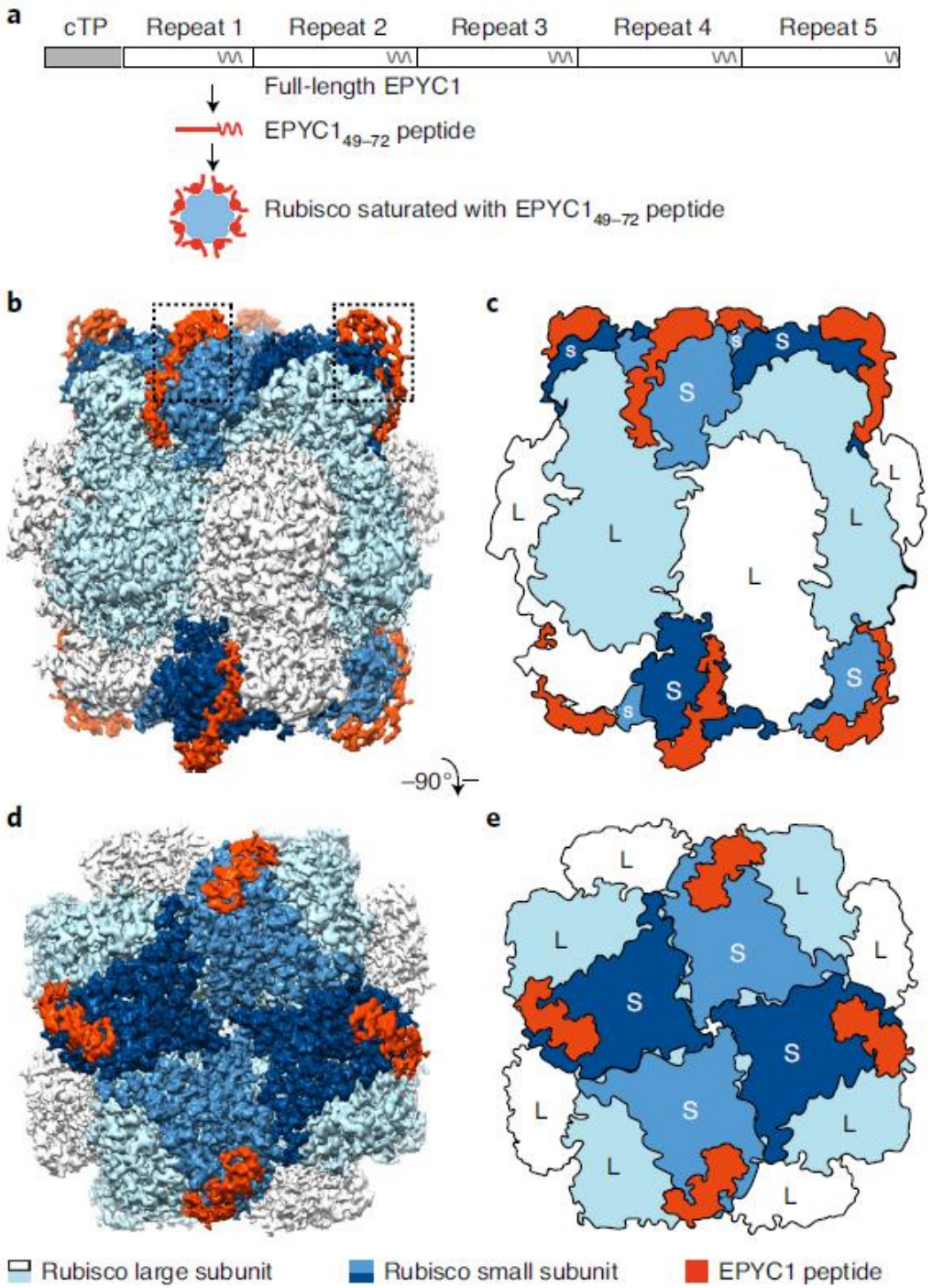

Fig. 2 | EPYC1 binds to Rubisco small subunits. a, Peptide EPYC1$_{49–72}$, corresponding to the first Rubisco-binding region of EPYC1, was incubated at saturating concentrations with Rubisco prior to single-particle cryo-electron microscopy. **b**–**e**, Density maps (**b**,**d**) and cartoons (**c**,**e**) illustrate the side views (**b**,**c**) and top views (**d**,**e**) of the density map of the EPYC1 peptide–Rubisco complex. The dashed boxes in **b** indicate the regions shown in Fig. 3a–f.

The pyrenoid, a Rubisco-containing organelle that enhances carbon fixation, mixes internally and undergoes phase transitions.

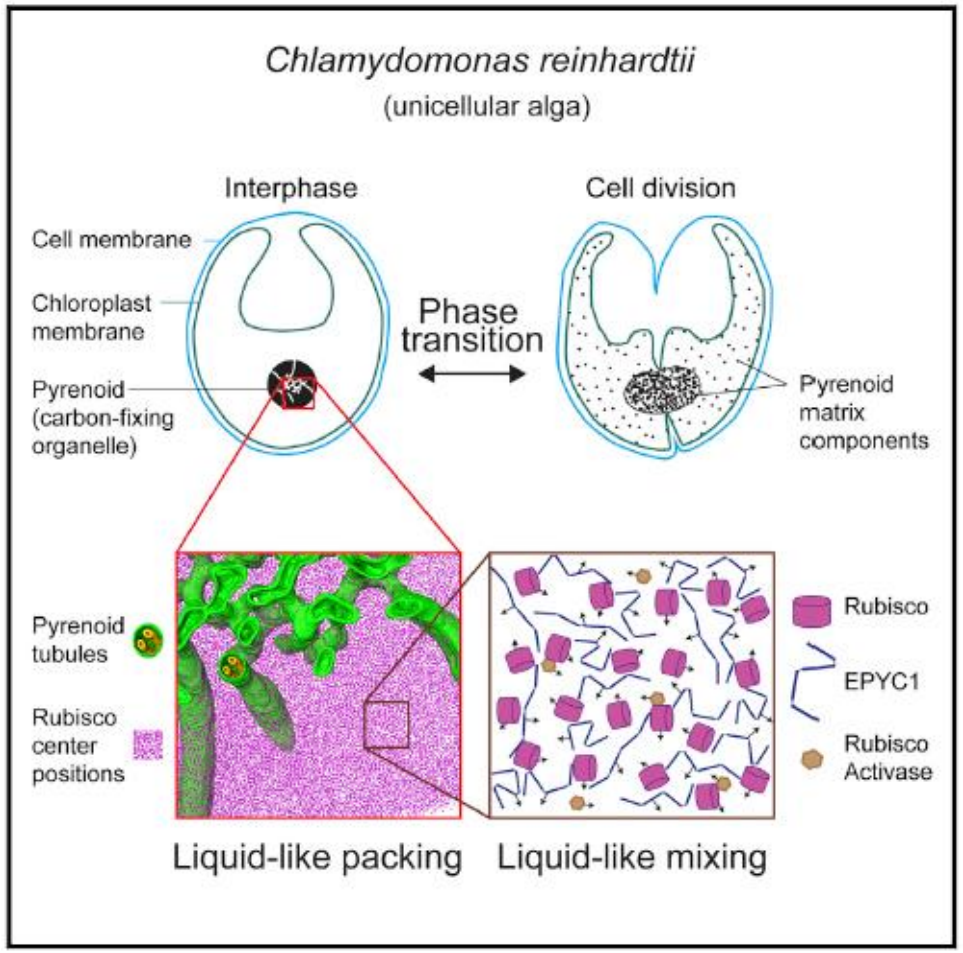

- The pyrenoid undergoes a reversible phase transition during cell division
- Modeling reveals a “magic number’’ effect that governs phase transitions

Bryophytes

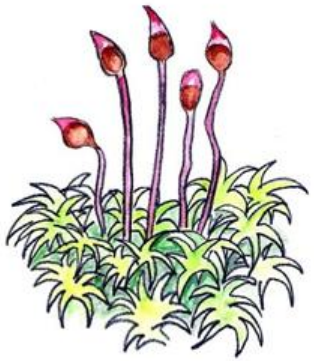

Moss

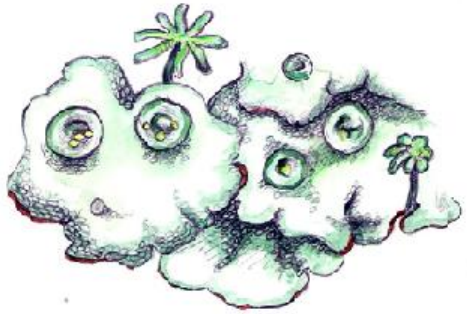

Liverwort

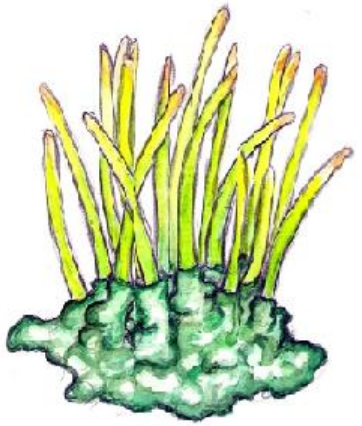

Hornwort

- About 100 species
- Similar to liverwort
- Hornlike sporophyte

PNAS

Hornwort pyrenoids, carbon-concentrating structures, evolved and were lost at least five times during the last 100 million years

Juan Carlos Villarreal[1] and Susanne S. Renner

Systematic Botany and Mycology, Department of Biology, University of Munich (LMU), Munich 80638, Germany

Edited by John Raven, University of Dundee, Dundee, United Kingdom, and accepted by the Editorial Board September 24, 2012 (received for review August

Pyrenoids are generally found in algae but they are also present in a group of plants called **hornworts**, suggesting they had an important **role during water-to-land transition in the green lineage**

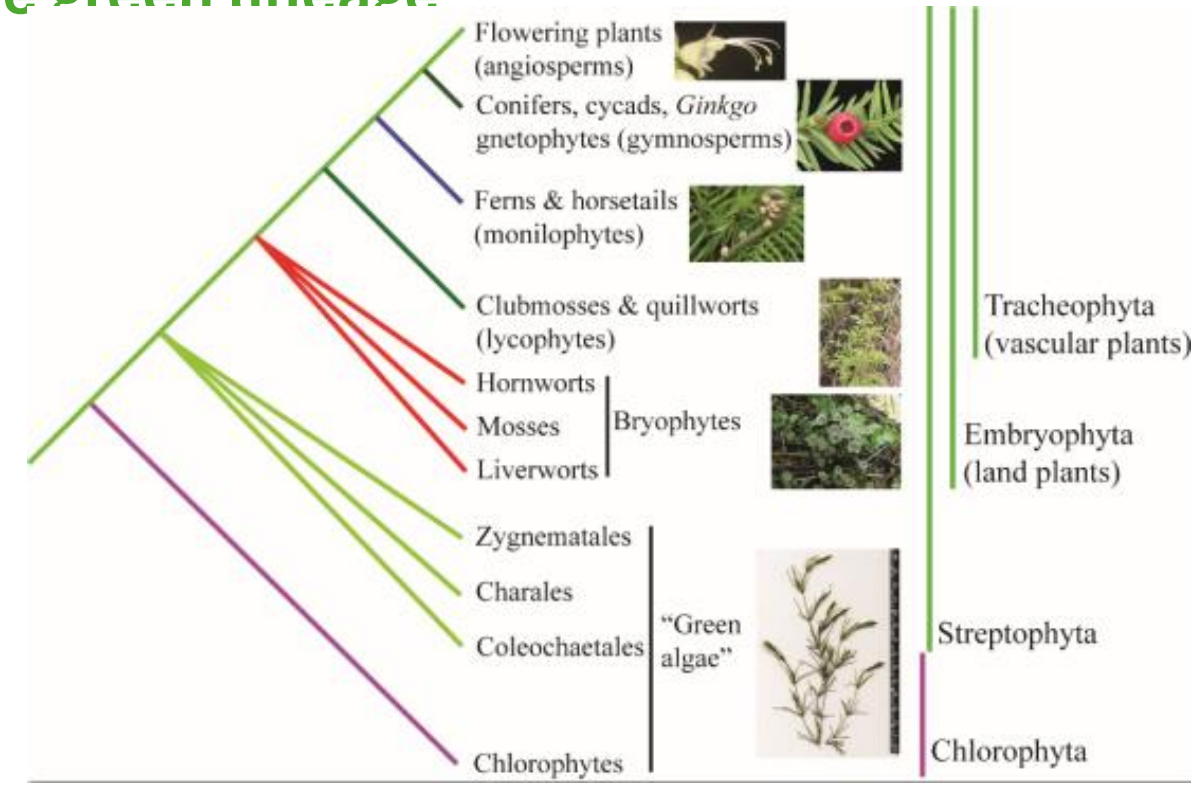

hornworts

Tree of life, the soltis lab

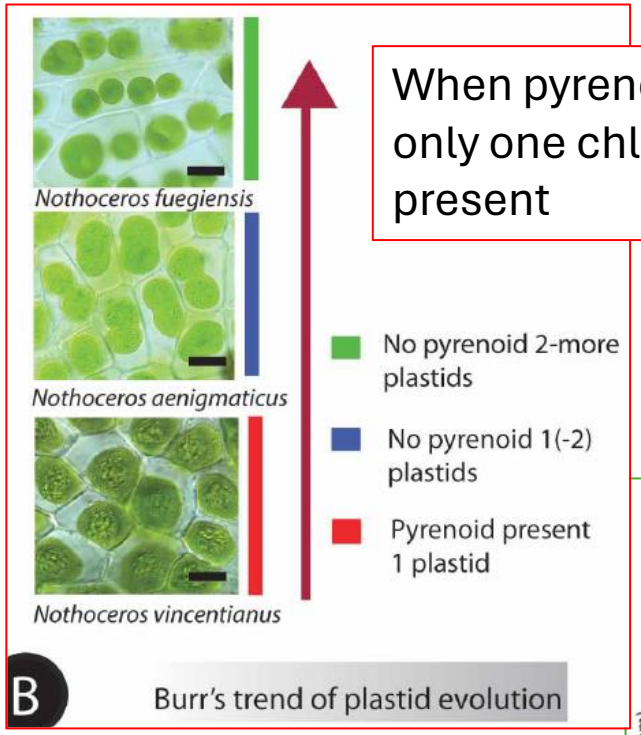

When pyrenoid is present, only one chloroplast is present

Pyrenoid evolution might be associated to water submergence more then [CO_2] in the atmosphere

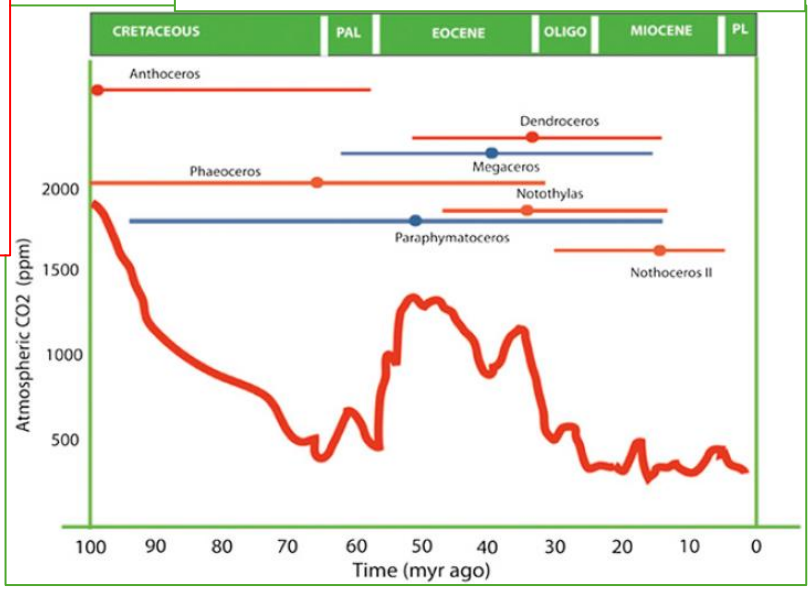

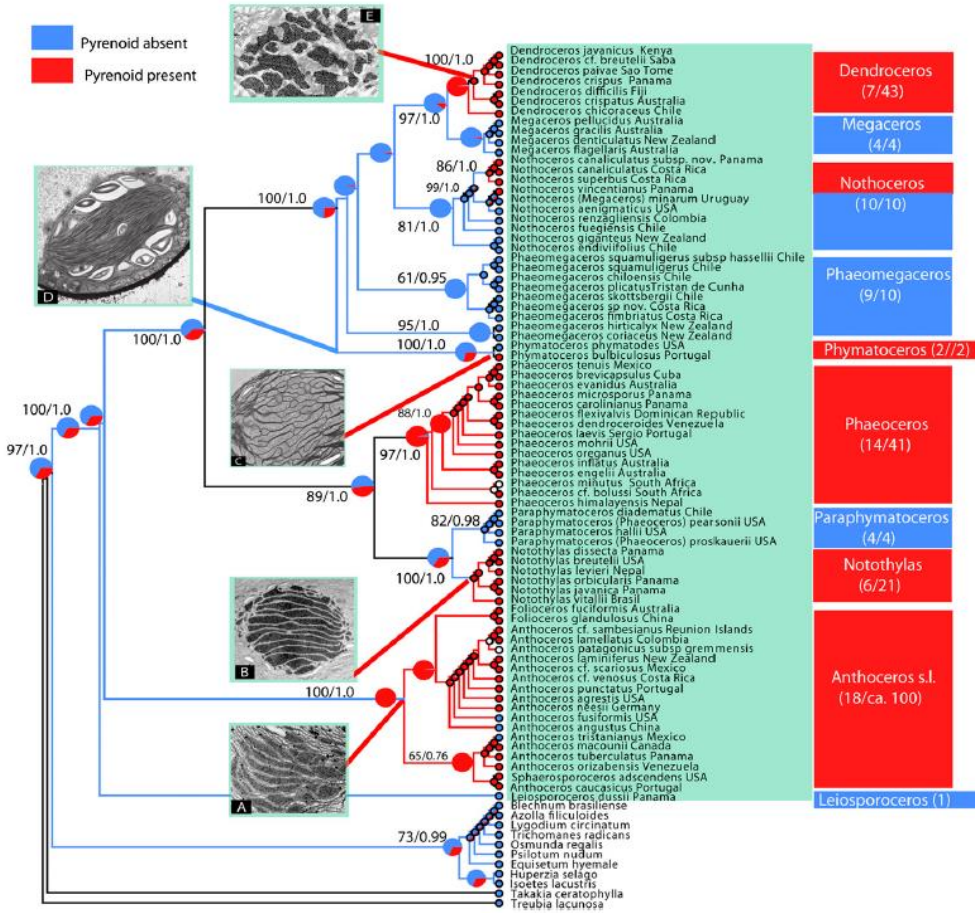

In hornwort, the pyrenoid is composed of subunits of various shapes

Gains and losses of the pyrenoid (and putative CCM) in hornworts.

Pyrenoids evolved from five to six times.

wrap-up

- Pyrenoids convert 30% of world CO_2 into organic carbon
- Pyrenoid-like structures could increase RUBISCO's performances in C3 plants
- High-throughput approaches allowed to identify proteins involved in pyrenoid formation and transmission to new generations
- The pyrenoid undergoes a reversible phase transition during cell division
- Hornworts as possible organisms to engineer plant pyrenoids

One potential approach for improving yields is the transfer of a CCM into higher plants to increase CO2-fixation rates

BBA - Molecular Cell Research 1868 (2021) 118949

Contents lists available at ScienceDirect

BBA - Molecular Cell Research

journal homepage: www.elsevier.com/locate/bbamcr

Review

Pyrenoids: CO_2-fixing phase separated liquid organelles

James Barrett [1], Philipp Girr [1], Luke C.M. Mackinder [*]

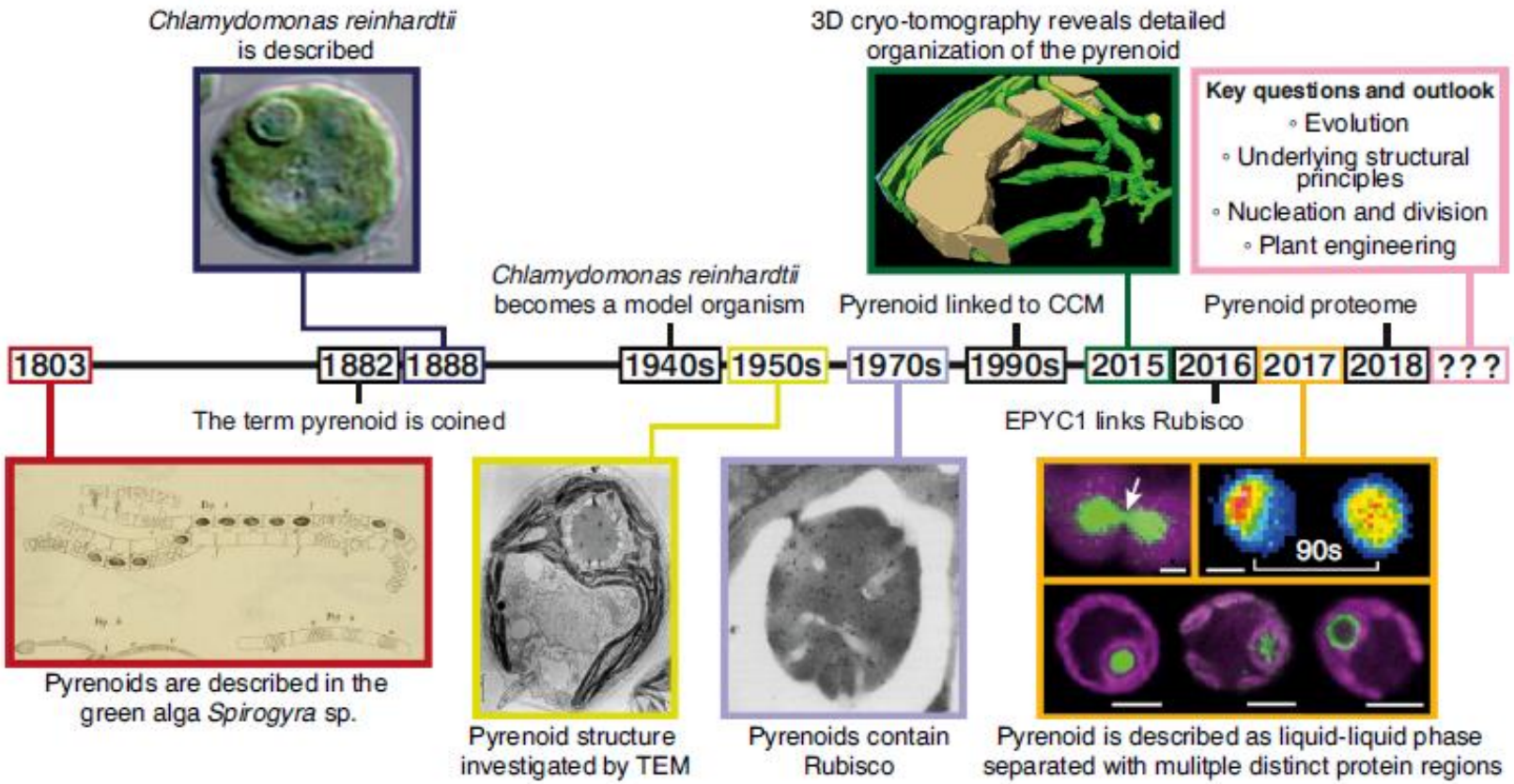

BBA - Molecular Cell Research 1868 (2021) 118949

Contents lists available at ScienceDirect

BBA - Molecular Cell Research

journal homepage: www.elsevier.com/locate/bbamcr

Review

Pyrenoids: CO_2-fixing phase separated liquid organelles

James Barrett [1], Philipp Girr [1], Luke C.M. Mackinder *

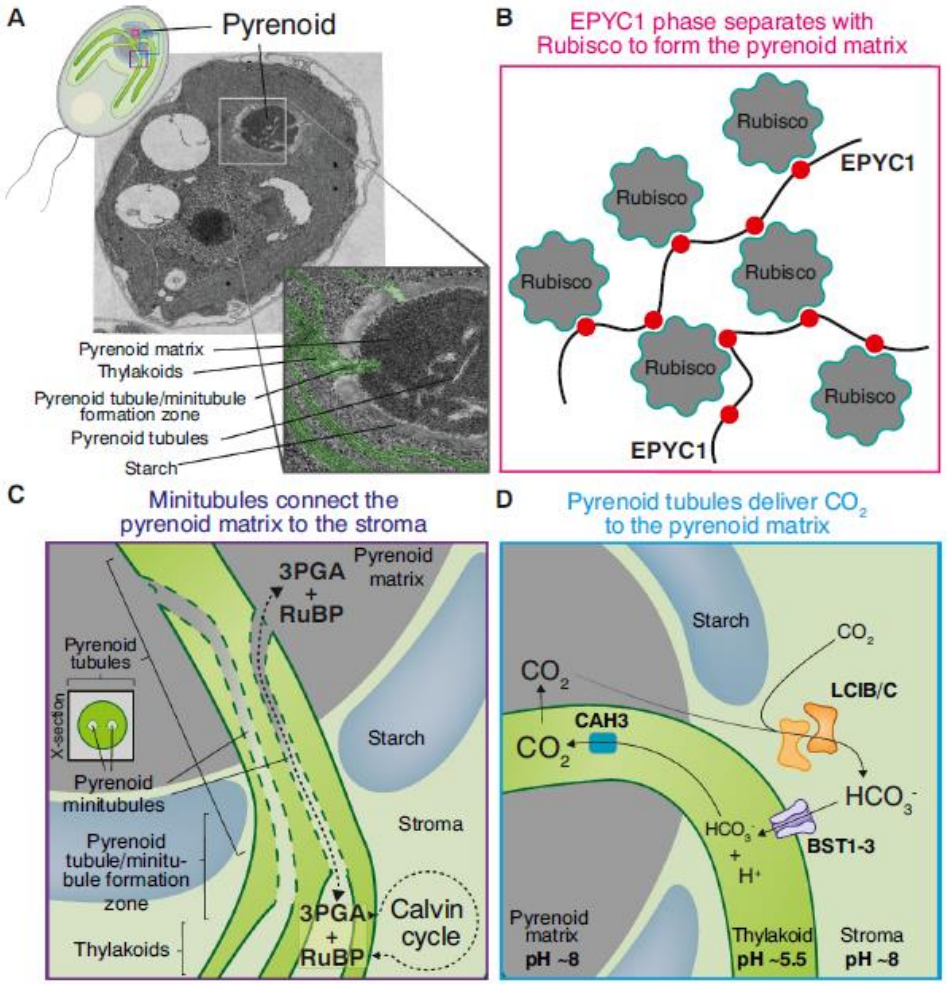

Fig. 4. The *Chlamydomonas* pyrenoid is at the heart of the CO_2 concentrating mechanism and enables efficient CO_2 fixation. A) TEM image of *Chlamydomonas reinhardtii* grown in light and under air levels of CO_2 where a complete pyrenoid is assembled. Zoom highlights key structural parts of the pyrenoid. Thylakoids false coloured green for clarity. Top left diagram is for orientation of panels B–D. B) The pyrenoid matrix is predominantly composed of Rubisco-EPYC1 condensate. Multiple Rubisco binding regions on EPYC1 enable complex coacervation with the Rubisco holoenzyme which is a hexadecameric assembly of 8 large and 8 small subunits. C) As thylakoids enter the pyrenoid they form pyrenoid tubules. Minitubules (dashed lines) form within the pyrenoid tubules and connect the pyrenoid matrix to the stroma. They are postulated to enable the large flux of metabolites in and out of the pyrenoid. Inset: cross-section (X-section) of minitubules within a pyrenoid tubule. D) Pyrenoid tubules are proposed to deliver CO_2 to Rubisco in the pyrenoid matrix. Current data supports that HCO_3^- enters from the stroma into the thylakoid lumen *via* bestrophin-like channels. In the acidic lumen HCO_3^- is converted to CO_2 *via* CAH3 and subsequently diffuses into the pyrenoid matrix. LCIB/LCIC is proposed to convert stromal CO_2 to HCO_3^- *via* active CO_2 uptake and CO_2 recapture from the pyrenoid. Minitubules are not shown for clarity.

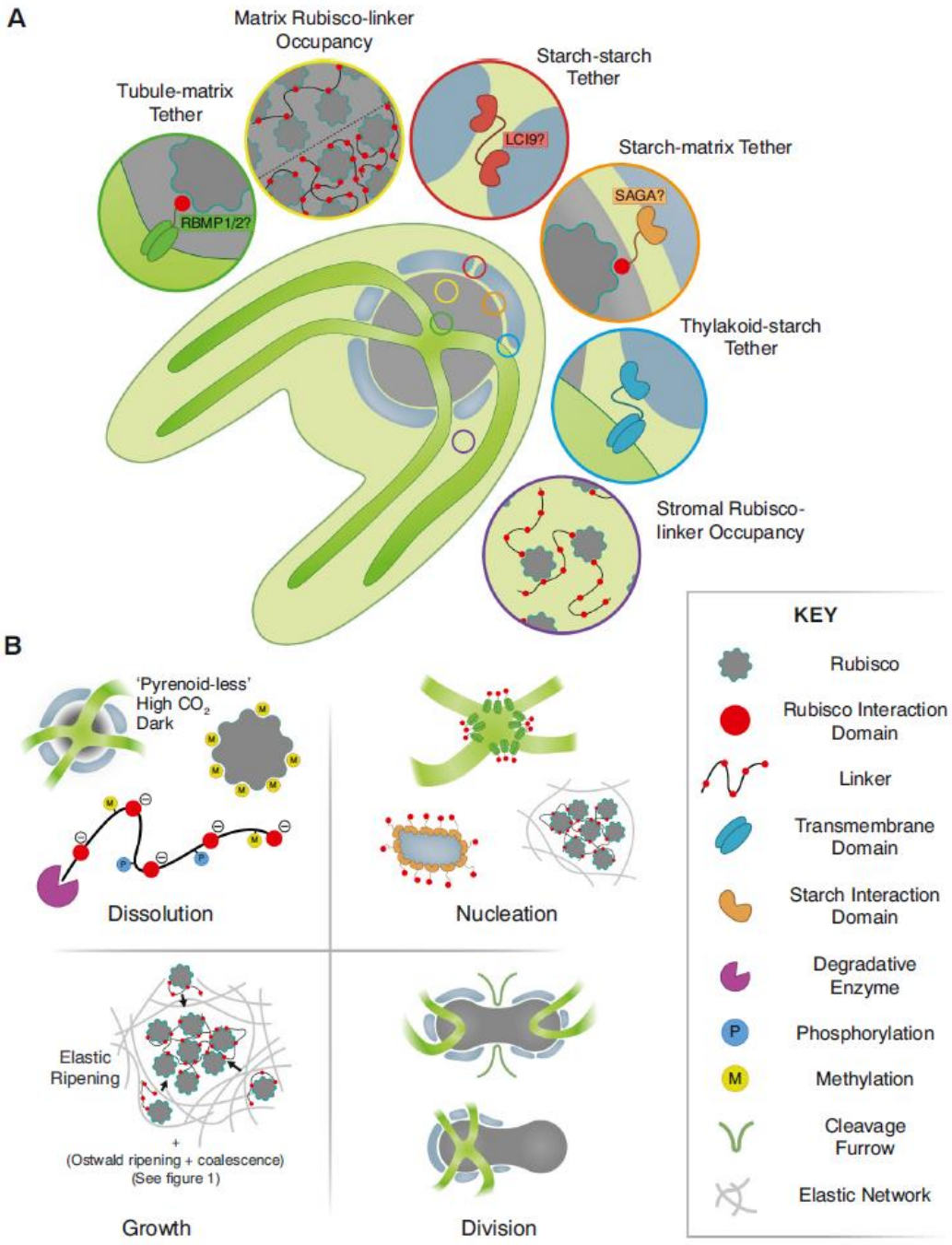

Fig. 5. Key unanswered questions in the *Chlamydomonas* pyrenoid. A) Molecular basis for pyrenoid localization at key ultrastructural features (clockwise from top left). A predicted pyrenoid tubule-enriched Rubisco-binding protein that could contribute to canonical positioning and localization of the pyrenoid matrix, as in B, perhaps contributed by RBMP1/2. The unknown occupancy of the Rubisco-linker interaction that underpins LLPS of the matrix, where the dashed line demarcates a low Rubisco, high linker occupancy and a high Rubisco, low linker occupancy scenario. A putative protein interaction that spans the inter-starch gaps in the sheath to tether adjacent plates, possibly fulfilled by LCI9, as highlighted in Mackinder et al. [80]. A starch-associated Rubisco-interacting protein that tethers the starch sheath to the matrix, possibly underpinning an alternative starch-centric nucleation model, as in B, perhaps performed by SAGA1/2 [42] among others. A putative thylakoid-associated, starch-binding protein that could explain the canonical positioning of the starch plates in pyrenoid-less strains. The uncharacterized occupancy and oligomeric state of the Rubisco-linker interaction in the dilute stromal phase. B) Potential control mechanisms underpinning the dynamics of the pyrenoid. Dissolution, clockwise from top left. The dissolved state of the pyrenoid, showing canonical positioning of the starch plates and retention of a portion of the matrix at the tubule intersection, possibly forming an interdependent assembly point. A methylated state of Rubisco that could disrupt linker interactions and contribute to dissolution. Potential linker perturbations that could contribute to phase transitions, including PTMs (phosphorylation and methylation) as well as degradation (concentration effect) and charge perturbation (pH and ion concentration). Nucleation, from top left. Tubule-enriched matrix tethers, that could nucleate a canonically positioned pyrenoid, consistent with A. Spontaneous nucleation at a region of low elastic density in the stroma. Starch-centric nucleation, seeded by starch-matrix tethers, consistent with A. Growth, multiple explanations for pyrenoid growth following *de novo* formation. Division, possibilities for ultrastructural distribution through cleavage furrow-induced pyrenoid fission.

nature COMMUNICATIONS

ARTICLE

https://doi.org/10.1038/s41467-020-20132-0 OPEN

Condensation of Rubisco into a proto-pyrenoid in higher plant chloroplasts

Nicky Atkinson[1], Yuwei Mao[1], Kher Xing Chan[2] & Alistair J. McCormick[1]

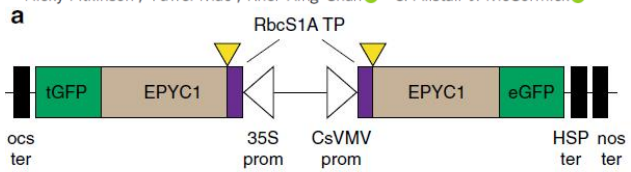

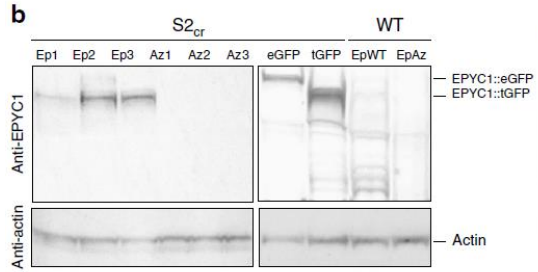

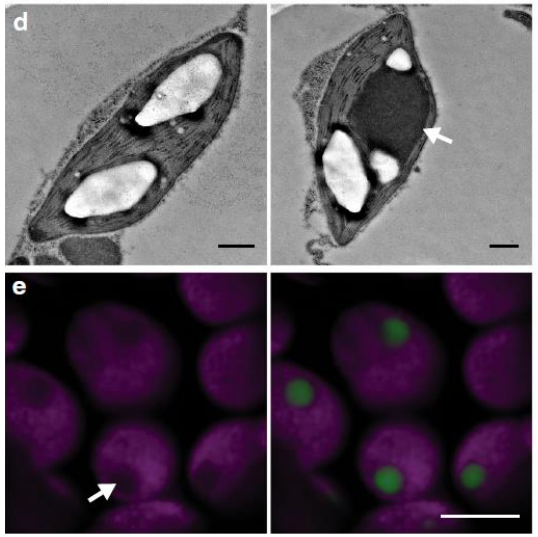

EPYC1 promotes pyrenoid formation in Arabidopsis

PERSPECTIVE | BIOCHEMISTRY

Putting the RuBisCO pieces together

TODD O. YEATES AND NICOLE M. WHEATLEY

SCIENCE • 8 Dec 2017 • Vol 358, Issue 6368 • pp. 1253-1254 • DOI: 10.1126/science.aar3107

RuBisCO assembly

Numerous plant chaperone genes were inserted into bacterial cells to promote the folding and assembly of the plant RuBisCO enzyme inside *E. coli*.

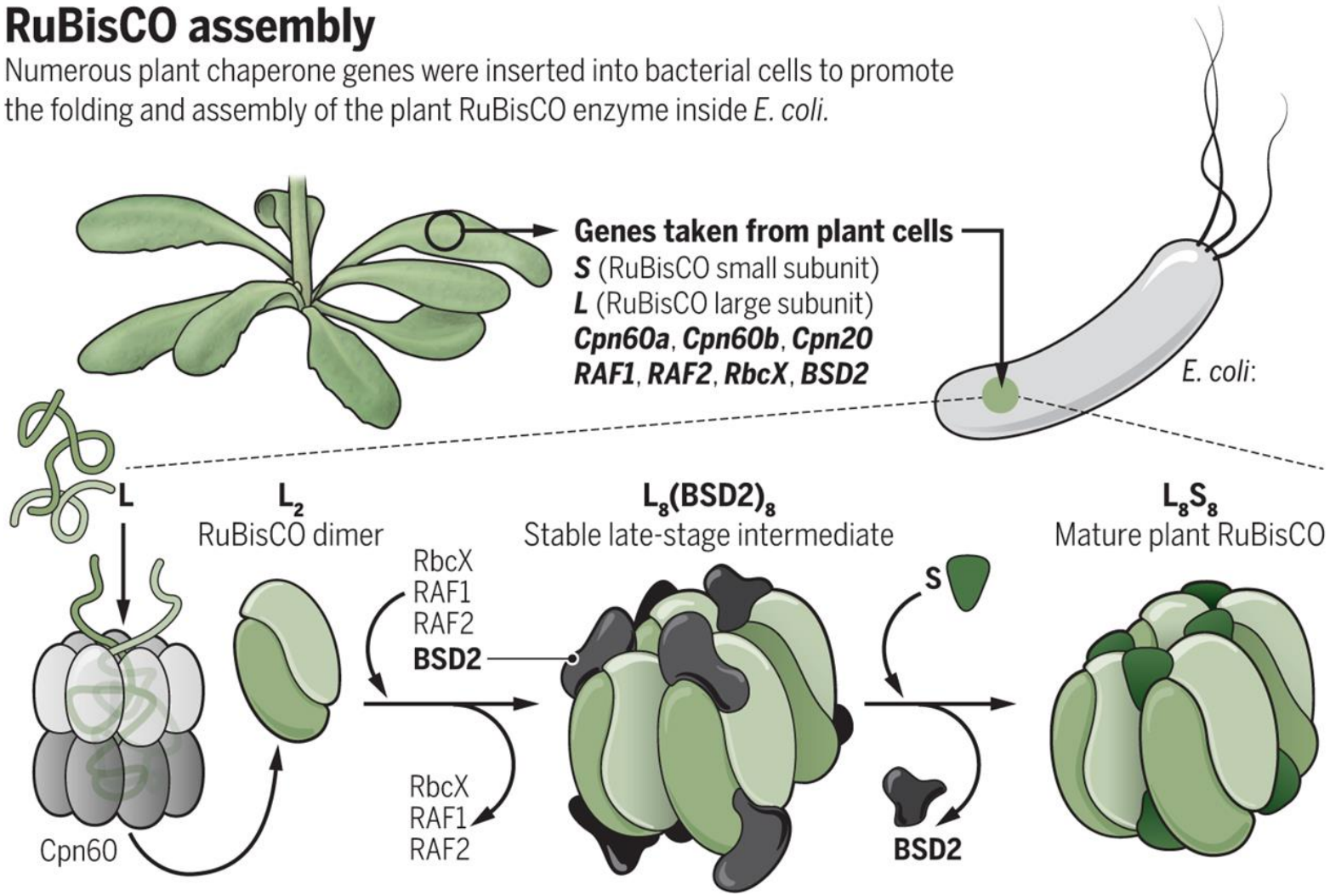

nature COMMUNICATIONS

ARTICLE

https://doi.org/10.1038/s41467-020-20132-0 OPEN

Condensation of Rubisco into a proto-pyrenoid in higher plant chloroplasts

Nicky Atkinson[1], Yuwei Mao[1], Kher Xing Chan[2] & Alistair J. McCormick[1]✉

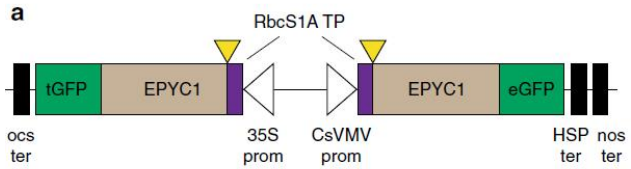

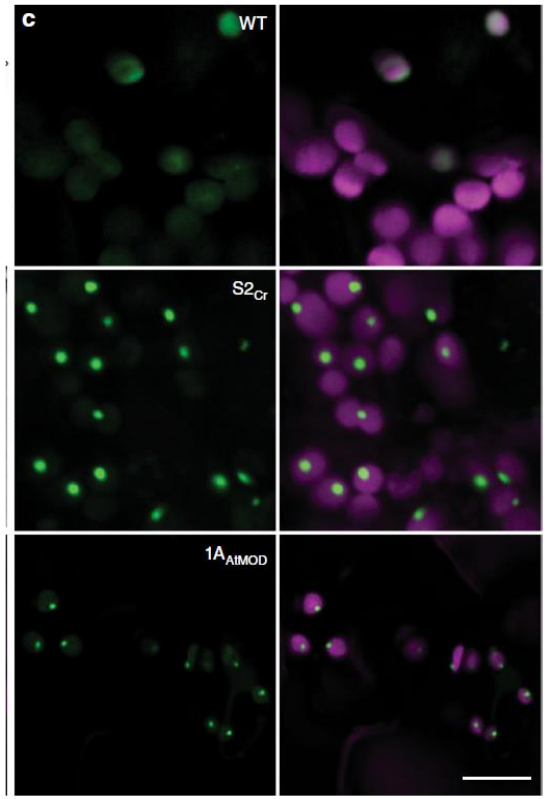

WT plants

Arabidopsis Rubisco mutant complemented with an SSU from Chlamydomonas ($S2_{Cr}$)

a native Arabidopsis SSU modified to contain the two α-helices necessary for pyrenoid formation from the Chlamydomonas SSU (1AAtMOD)

nature COMMUNICATIONS

ARTICLE

https://doi.org/10.1038/s41467-020-20132-0 OPEN

Condensation of Rubisco into a proto-pyrenoid in higher plant chloroplasts

Nicky Atkinson[1], Yuwei Mao[1], Kher Xing Chan[2] & Alistair J. McCormick[1]✉

Arabidopsis Chlamydomonas

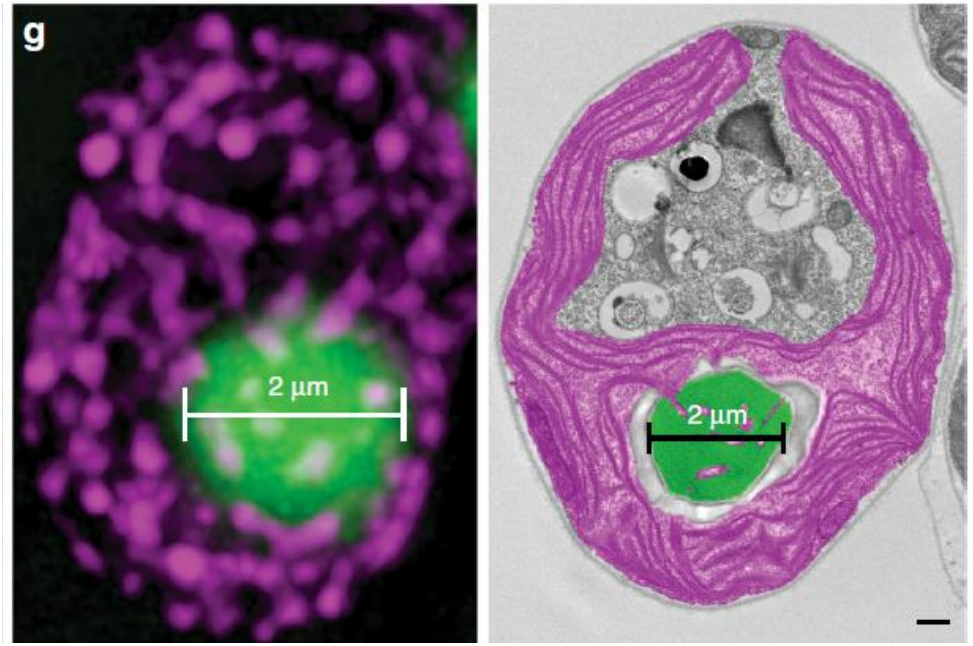

In planta condensates behave like liquid–liquid phase-separated microcompartments.

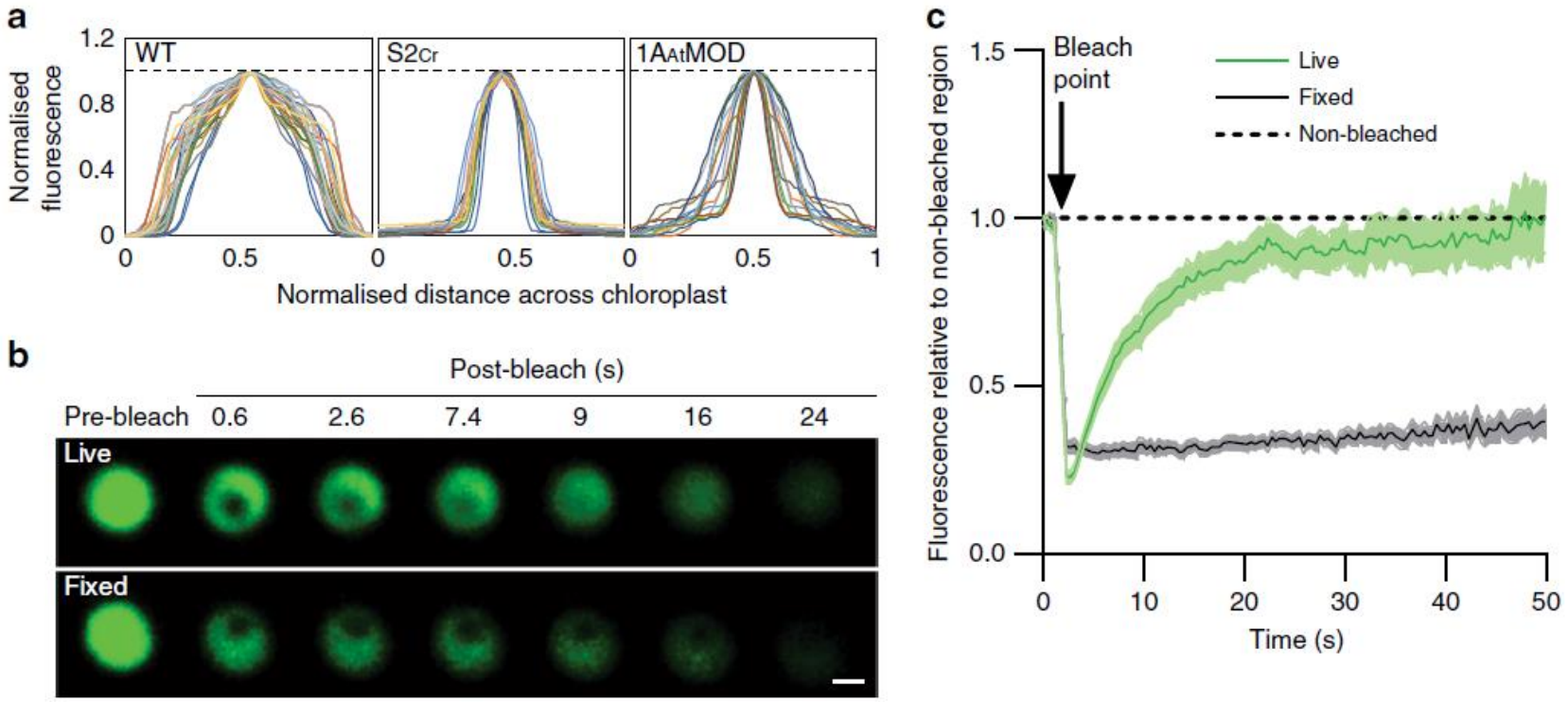

- Fixed with fomaldehyde

Immunogold labelling

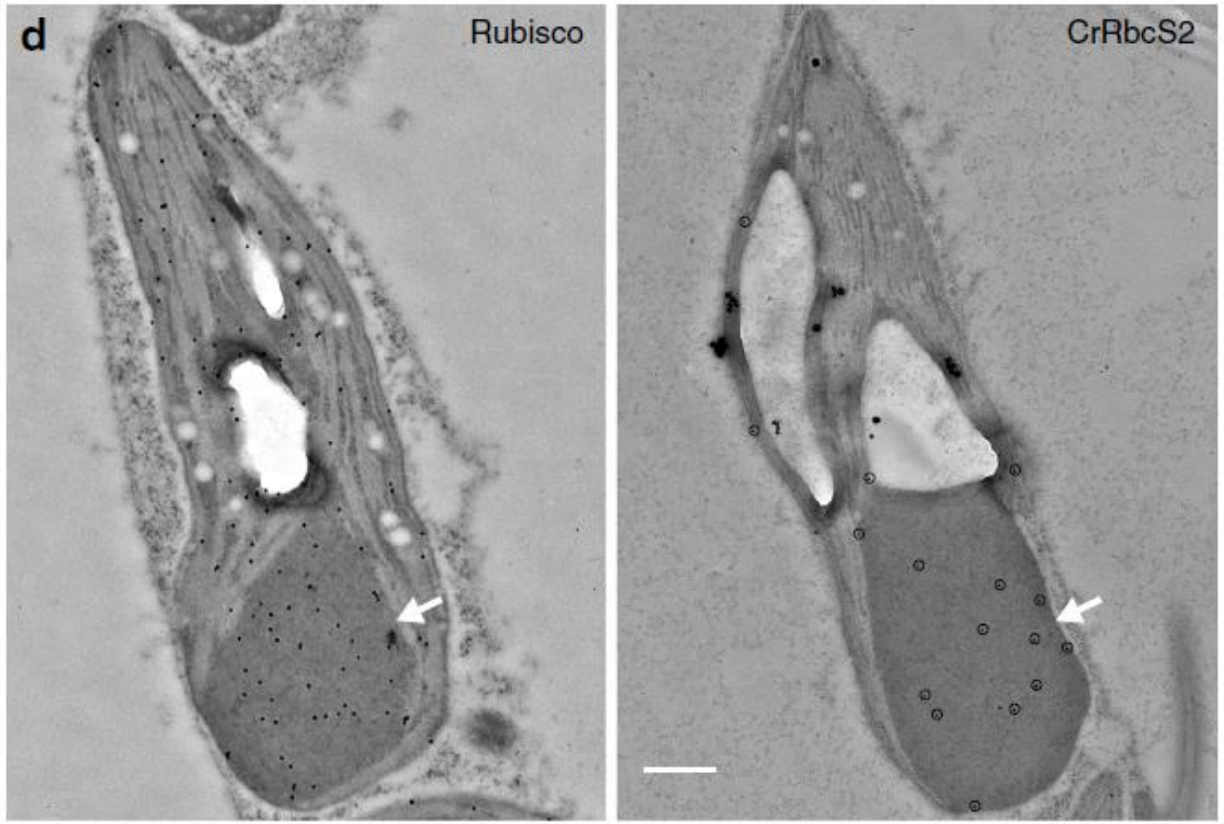

EPYC1-mediated condensation of Rubisco has no negative impact on growth and photosynthesis.

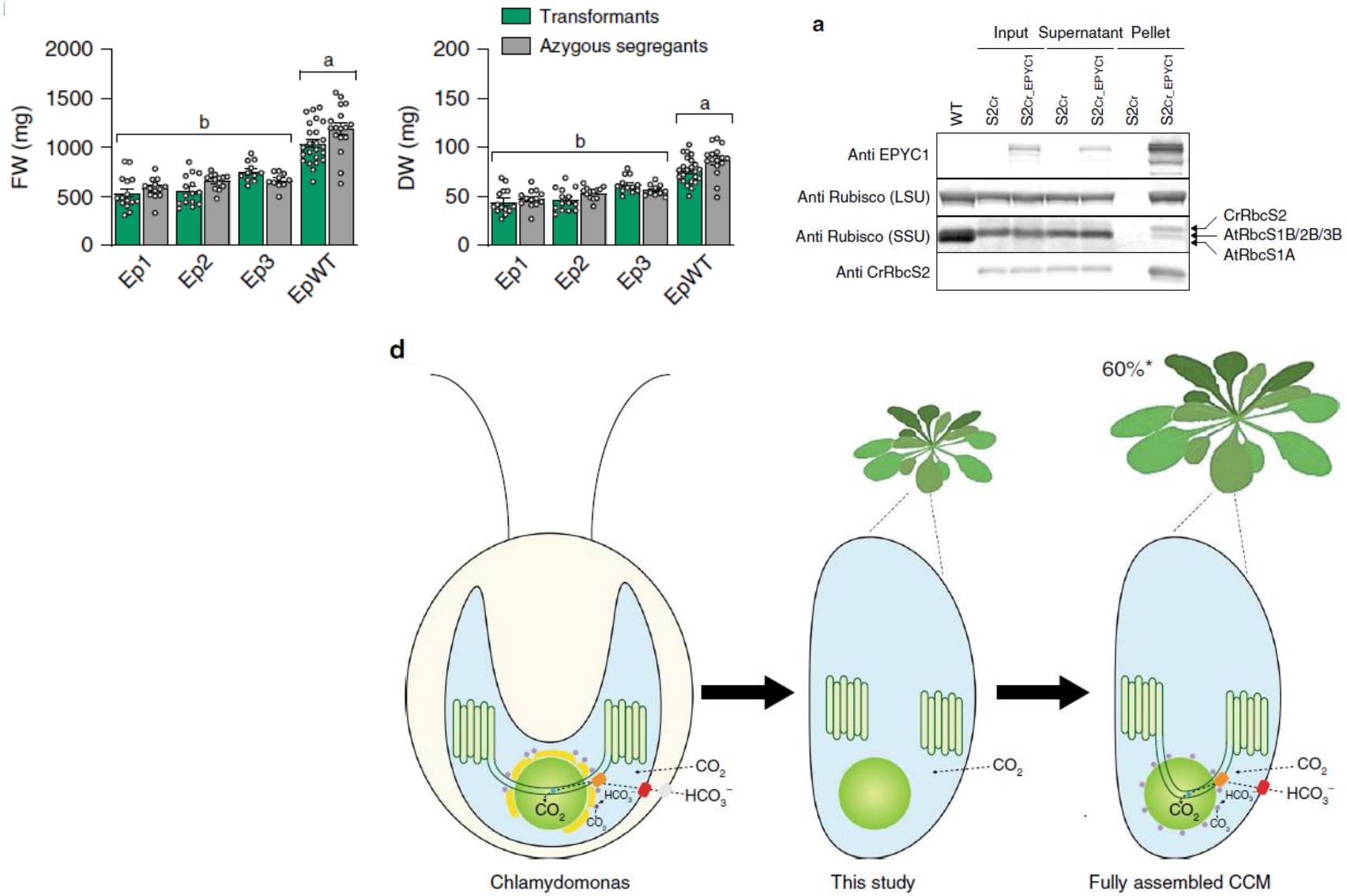

The following step

Photosynthesis Research (2023) 156:181–192
https://doi.org/10.1007/s11120-022-00996-7

ORIGINAL ARTICLE

A pyrenoid-localized protein SAGA1 is necessary for Ca^{2+}-binding protein CAS-dependent expression of nuclear genes encoding inorganic carbon transporters in *Chlamydomonas reinhardtii*

Daisuke Shimamura[1] · Takashi Yamano[1] · Yuki Niikawa[1] · Donghui Hu[1] · Hideya Fukuzawa[1]

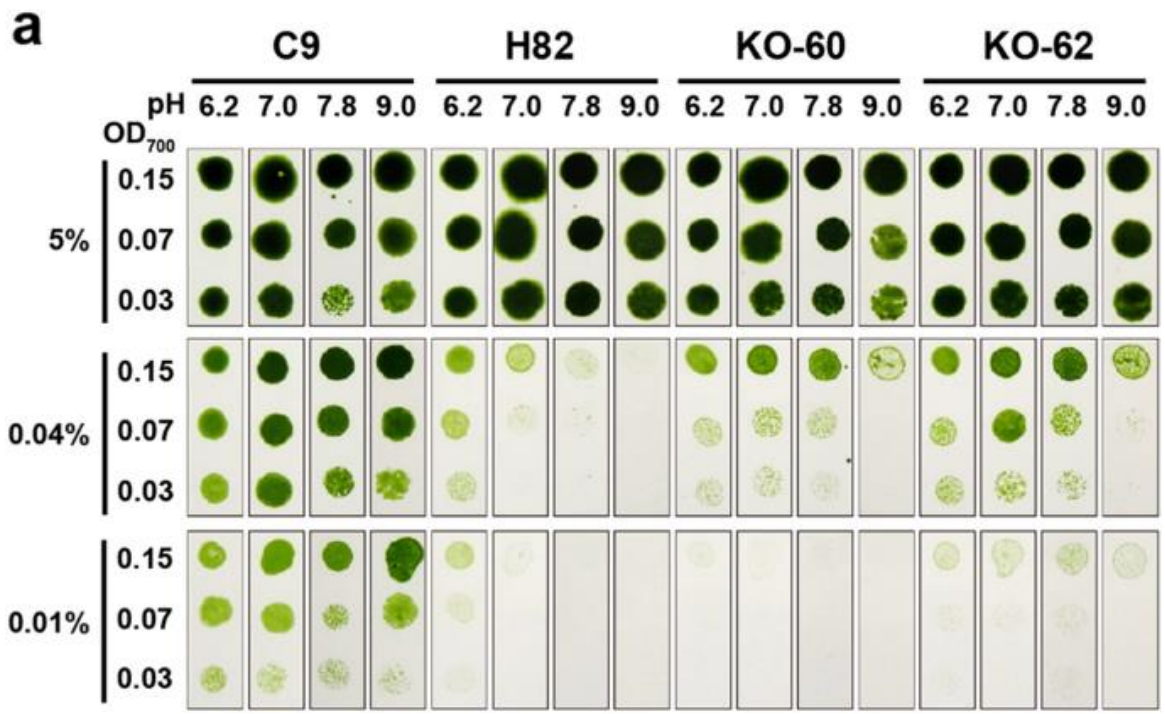

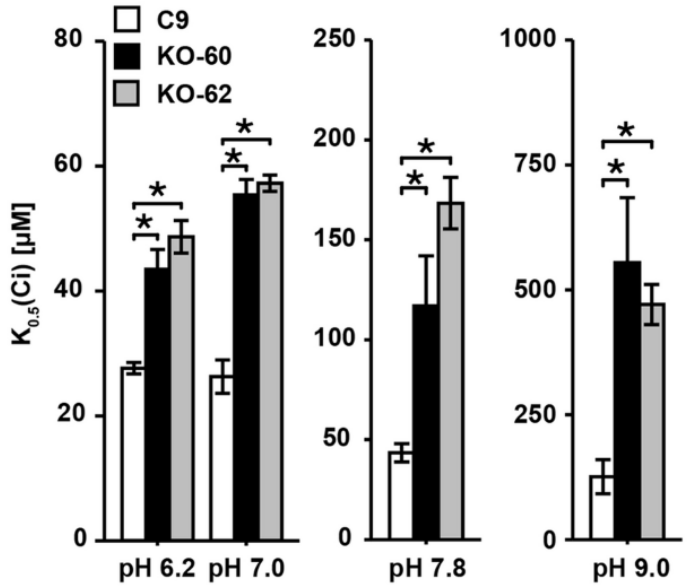

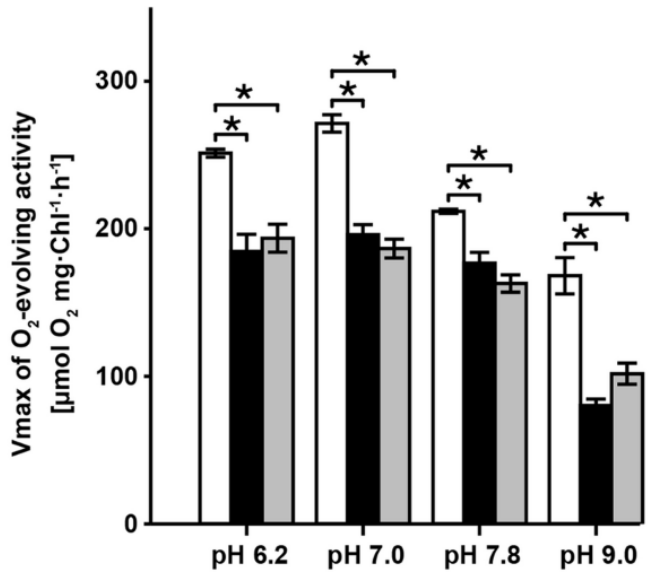

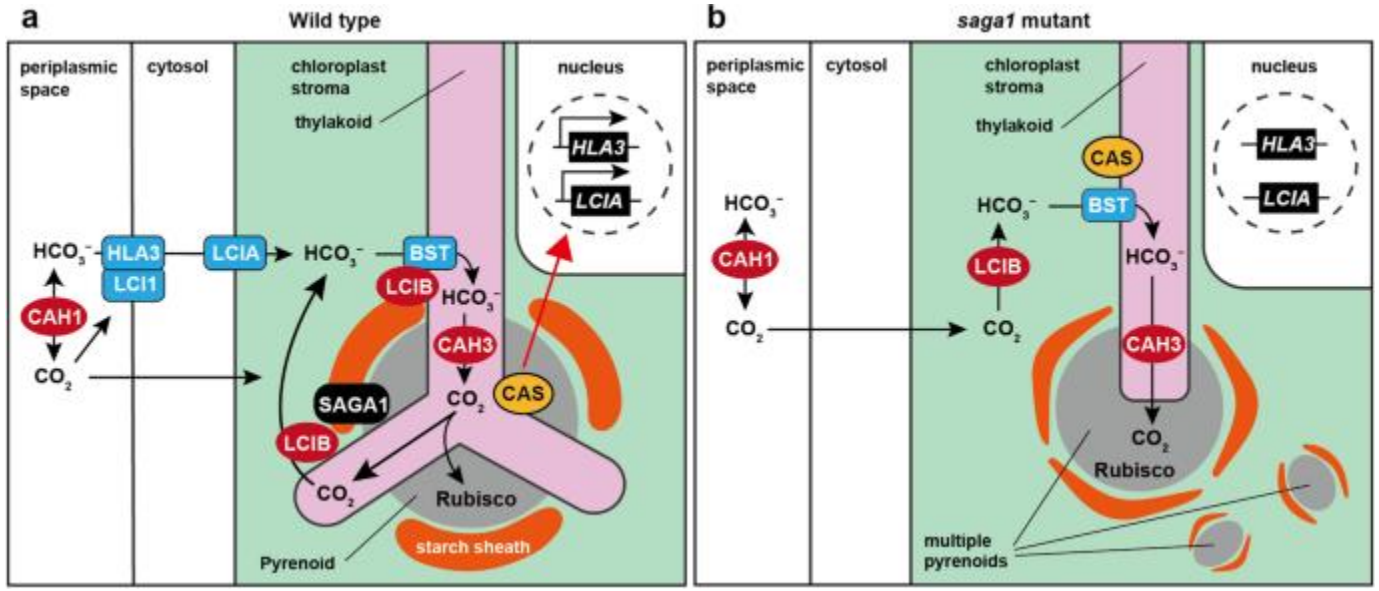
a
Wild type
periplasmic space
cytosol
chloroplast stroma
thylakoid
nucleus
HLA3
LCIA
HCO3-
HLA3
LCI1
LCIA
HCO3-
BST
LCIB
HCO3-
CAH1
CAH3
CO2
CAS
SAGA1
LCIB
CO2
Rubisco
CO2
Pyrenoid
starch sheath
b
saga1 mutant
periplasmic space
cytosol
chloroplast stroma
thylakoid
nucleus
CAS
HCO3-
BST
HCO3-
CAH1
LCIB
HCO3-
CO2
CO2
CAH3
CO2
Rubisco
multiple pyrenoids

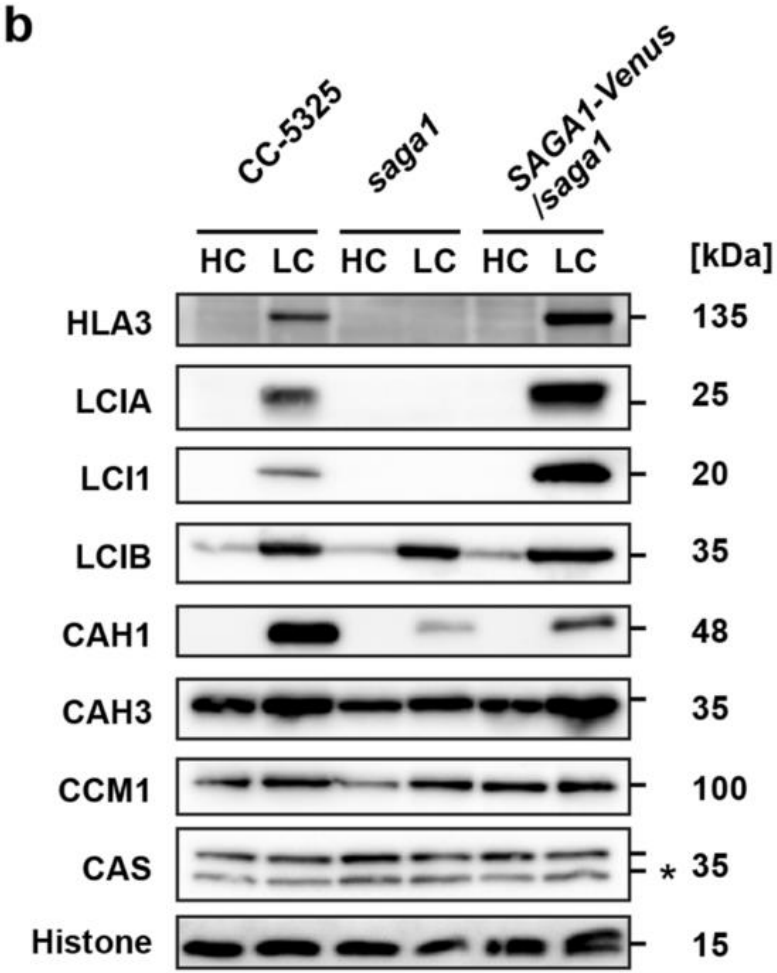
b
CC-5325
saga1
SAGA1-Venus /saga1
HC LC HC LC HC LC
[kDa]
HLA3
135
LCIA
25
LCI1
20
LCIB
35
CAH1
48
CAH3
35
CCM1
100
CAS
* 35
Histone
15

PNAS RESEARCH ARTICLE | PLANT BIOLOGY

SAGA1 and SAGA2 promote starch formation around proto-pyrenoids in Arabidopsis chloroplasts

Nicky Atkinson[a,b], Rhea Stringer[c], Stephen R. Mitchell[a], David Seung[c,1], and Alistair J. McCormick[a,b,1]

uly 27, 2023; accepted December 11, 2023

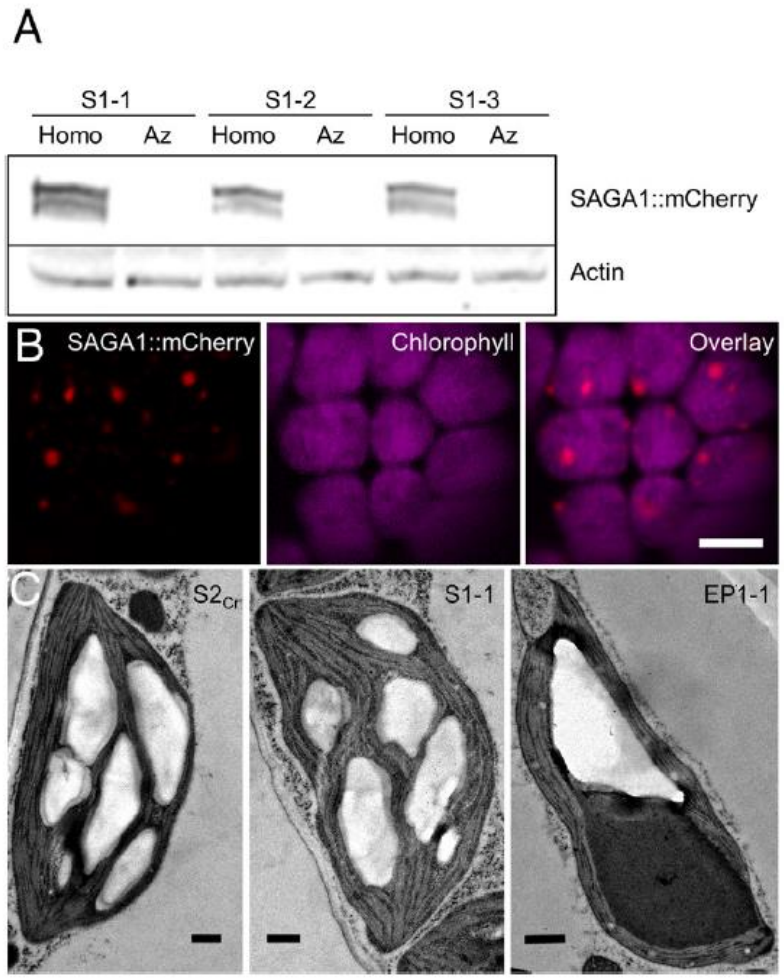

- SAGA1::mCherry localizes to the proto-pyrenoid and forms a ring around EPYC1::GFP.
- Representative TEM images of EP1S1-1 chloroplasts with atypical spherical enclosed (E), adjacent (A), and typical stromal (S) starch granule labeled. The lighter-staining pattern is highlighted with an asterisk. (Scale bar, 0.5 µm.)

PNAS RESEARCH ARTICLE | PLANT BIOLOGY

SAGA1 and SAGA2 promote starch formation around proto-pyrenoids in Arabidopsis chloroplasts

Nicky Atkinson[a,b], Rhea Stringer[c], Stephen R. Mitchell[a], David Seung[c,1], and Alistair J. McCormick[a,b,1]

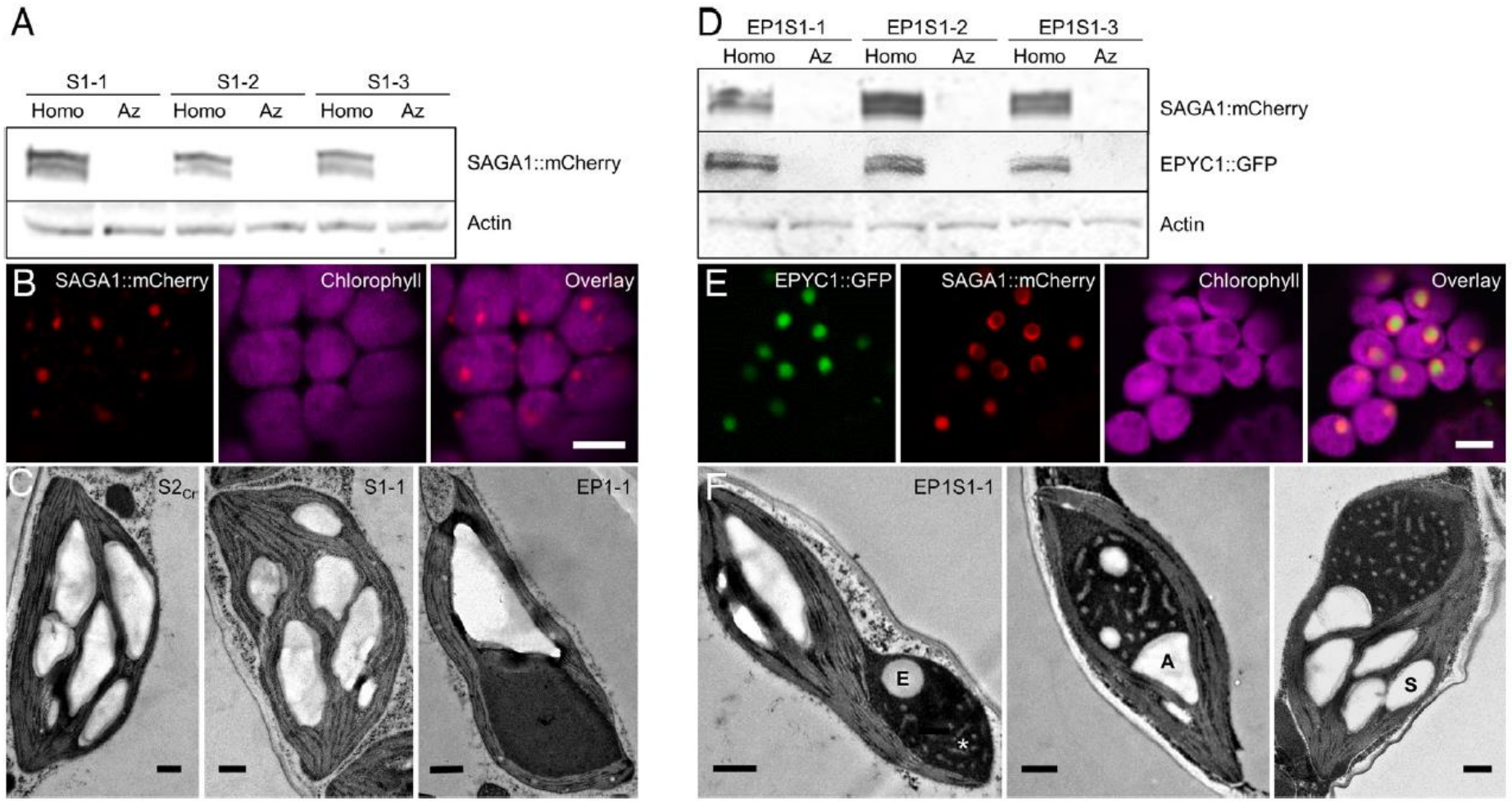

- SAGA1::mCherry localizes to the proto-pyrenoid and forms a ring around EPYC1::GFP.
- Representative TEM images of EP1S1-1 chloroplasts with atypical spherical enclosed (E), adjacent (A), and typical stromal (S) starch granule labeled. The lighter-staining pattern is highlighted with an asterisk. (Scale bar, 0.5 μm.)

B

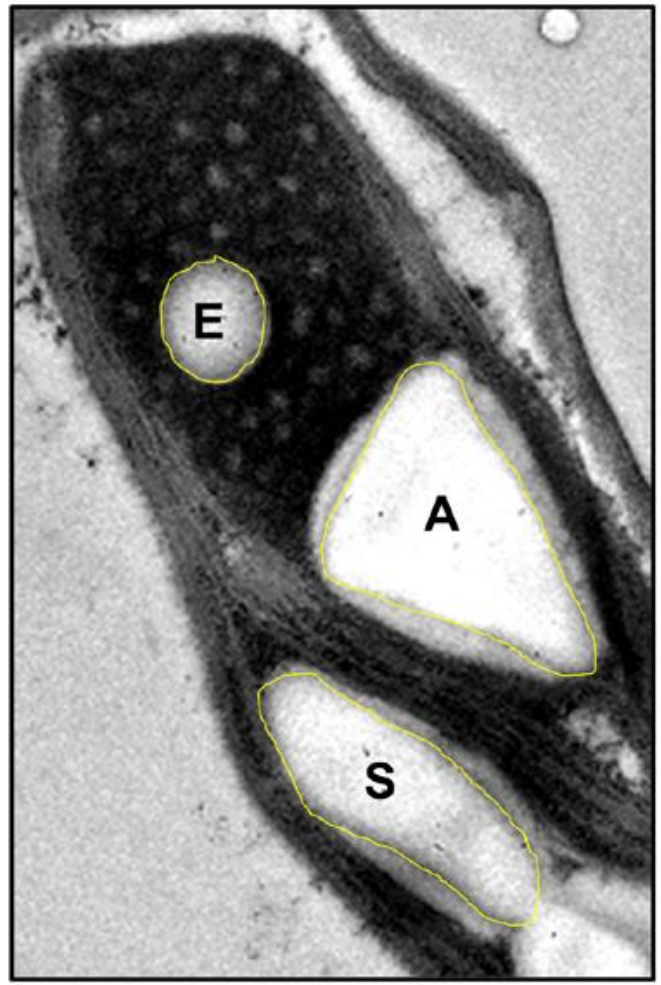

E. Enclosed (circularity = 0.96)
A. Adjacent (circularity = 0.72)
S. Stromal (circularity = 0.63)

C

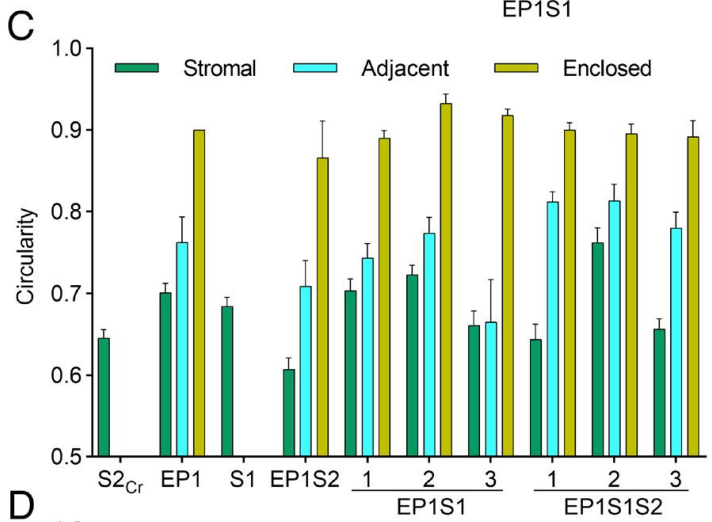

D

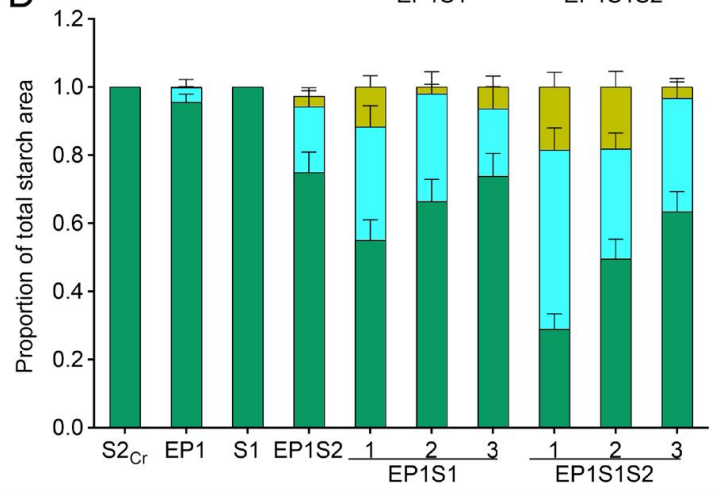

E

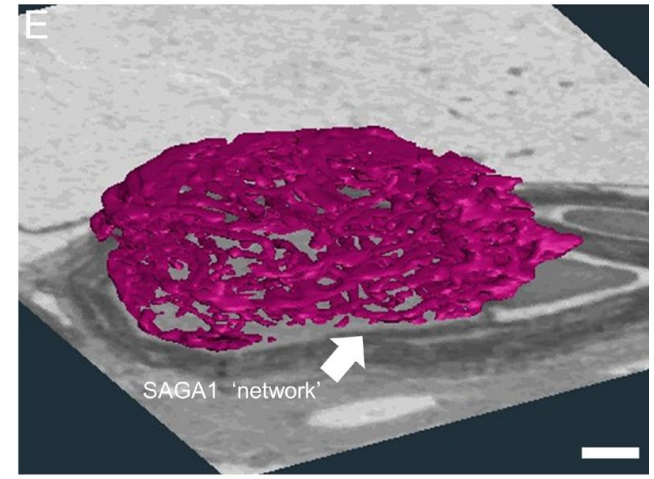

F

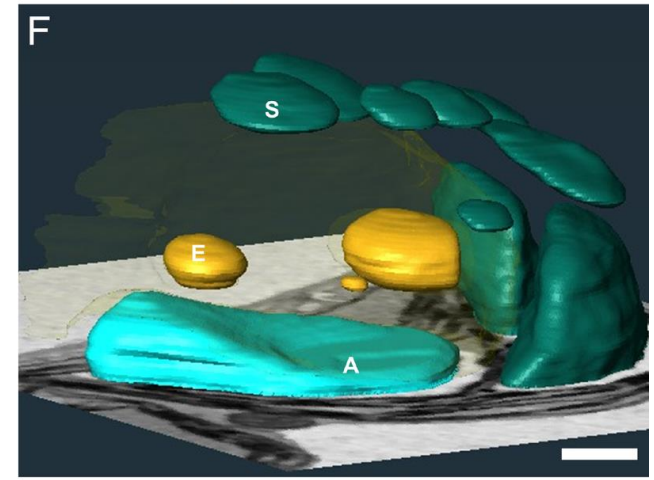

G

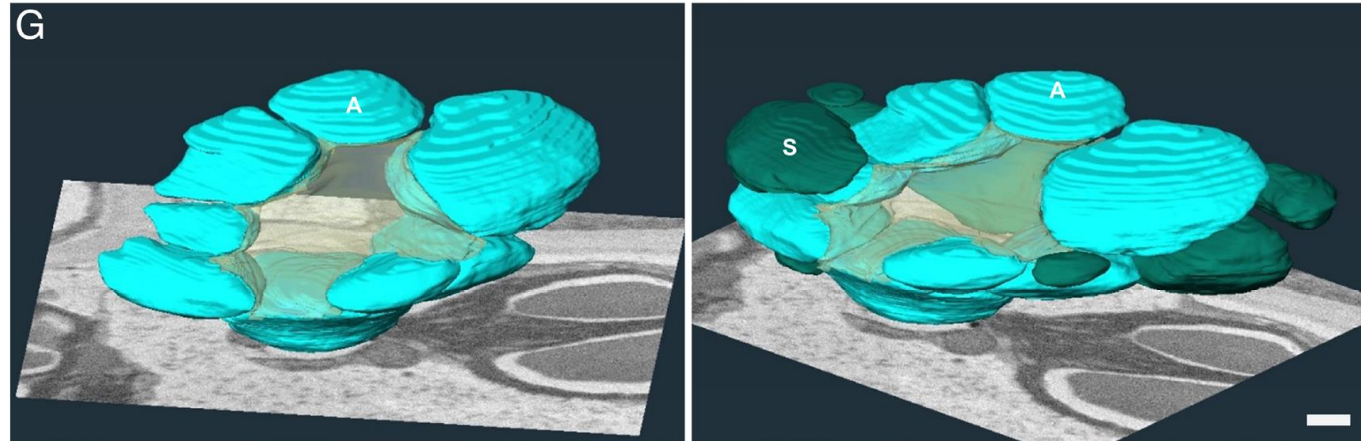

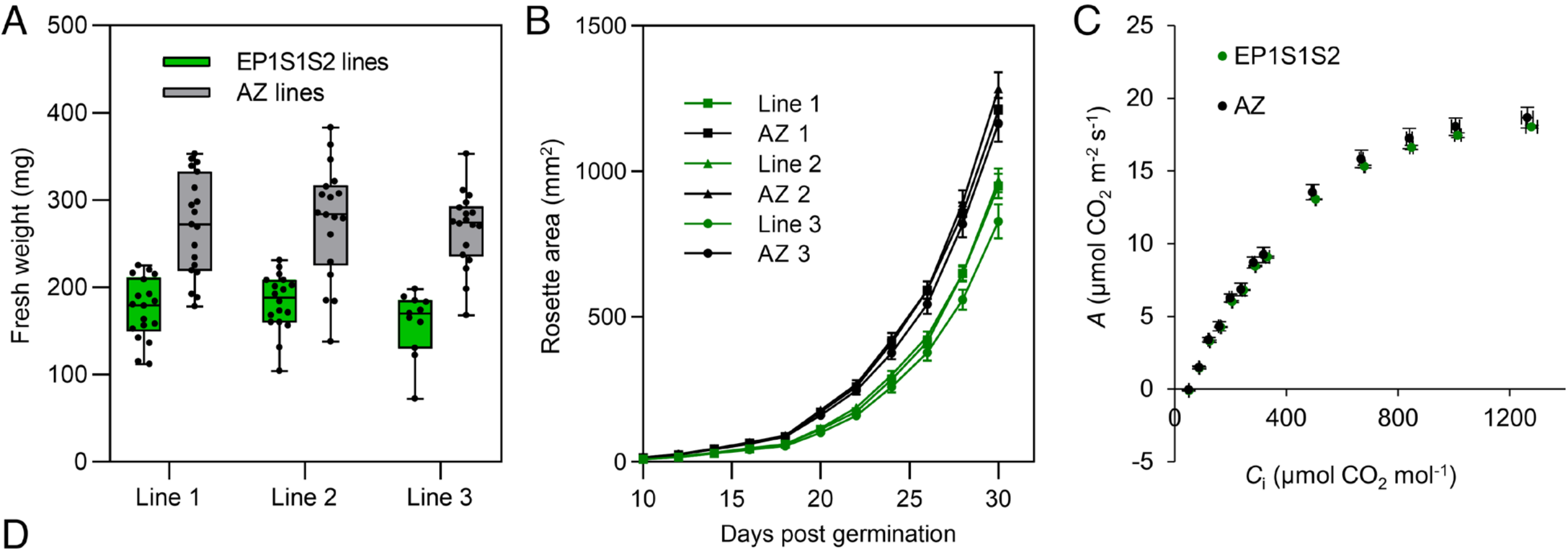

Growth is reduced but not photosynthetic performance in EP1S1S2 lines. (A) Fresh weight of EP1S1S2 lines and their azygous (Az) segregants 32 d after germination. The S2Cr background line was used as a control for line 1 as the Az segregant line had consistent germination and growth problems. (B) Rosette expansion for S1 and EP1S1 lines measured over 30 d postgermination.

New frontiers are coming

Origin of Chloro-Nucleo communication

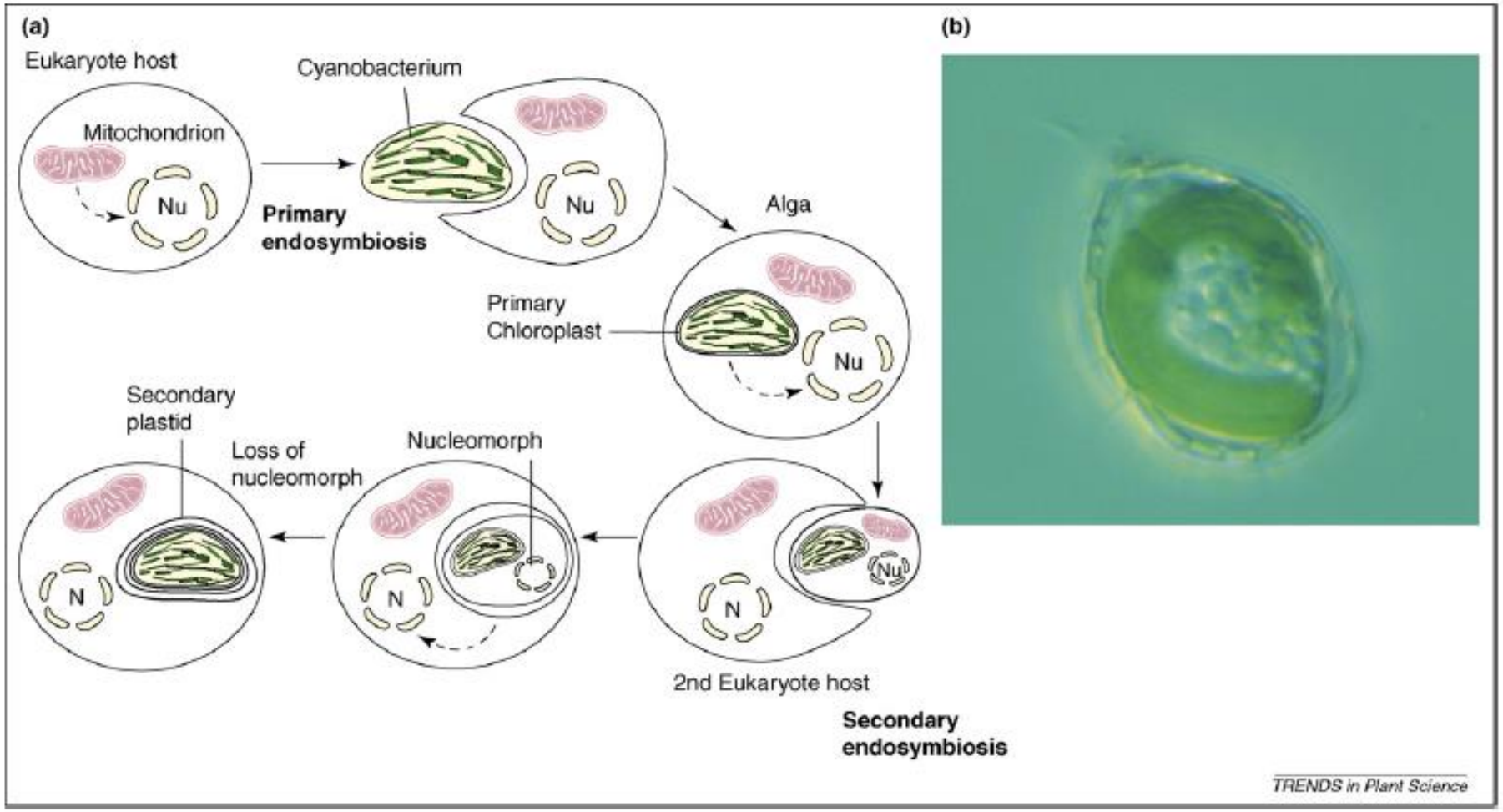

Figure 1. Origin of plastids by primary and secondary endosymbiosis. **(a)** Acquisition of a cyanobacterium by primary endosymbiosis, and subsequent secondary endosymbiotic acquisition of the resulting eukaryotic alga. The intermediate algal nucleus (Nu) forms the nucleomorph, which is subsequently reduced. N indicates the nucleus of the second eukaryote host. Broken arrows indicate gene transfer. **(b)** Photomicroscope image of a cell of *Paulinella*. Cell length is ~25 μm. The photograph shows the scales of the theca, a filopodium, and a large, dividing photosynthetic body or 'chromatophore'. Photograph kindly supplied by Birger Marin.

Nuclear genome

Chloroplast genom

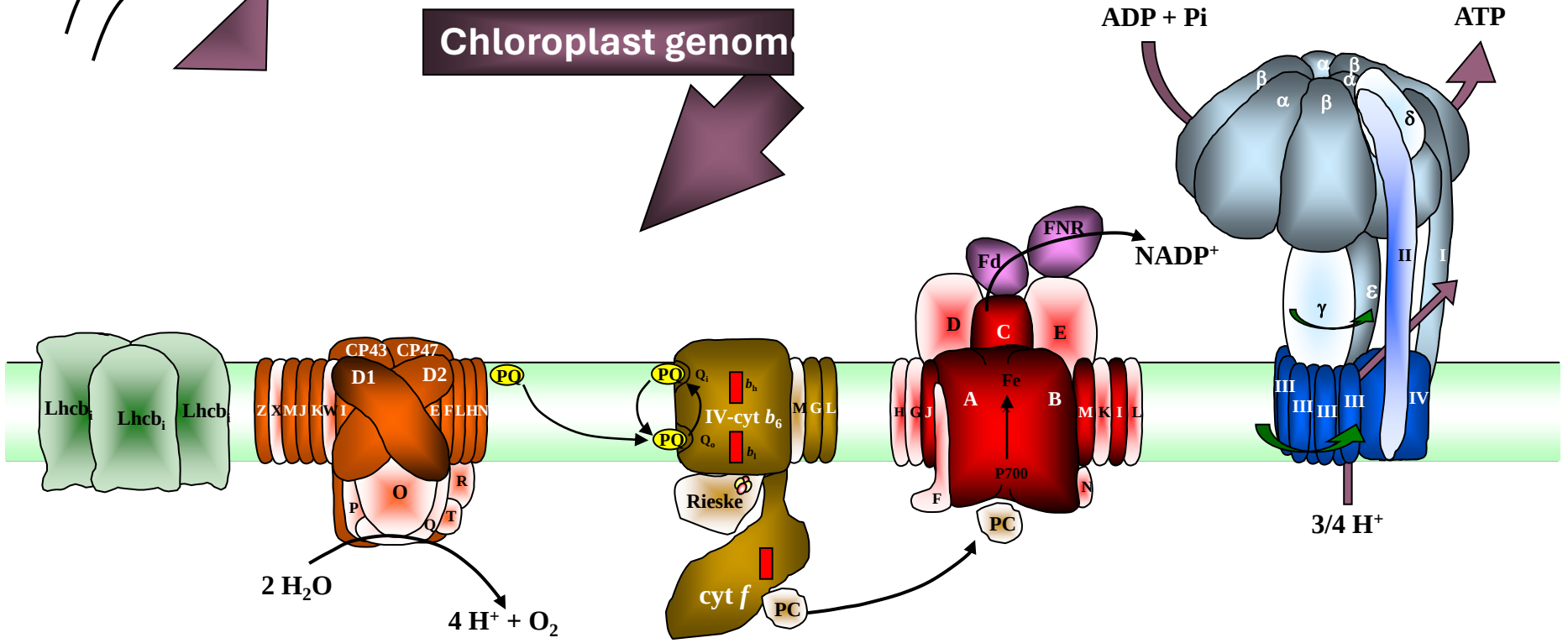

Chloroplast protein regulation

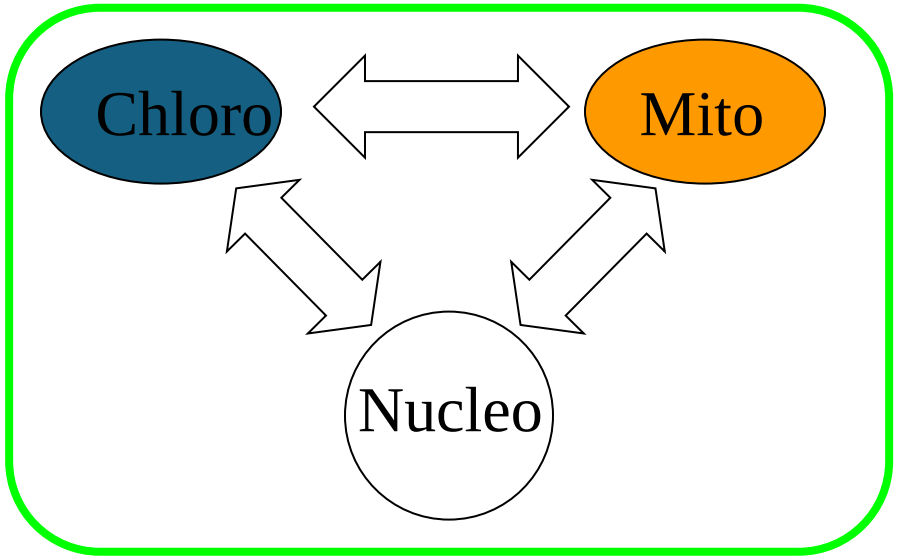

- Chloroplast genome only contains 120 genes
- Chloroplast proteome about 2500
- Synthesis of chloroplast proteins during acclimation is a concerted mechanism between plastid and nuclear genome

So what?

Which signals induce acclimation?

- PlastiQuinone Redox State (PQ)
- Chemicals (Chlorophyll precursors)
- ROS

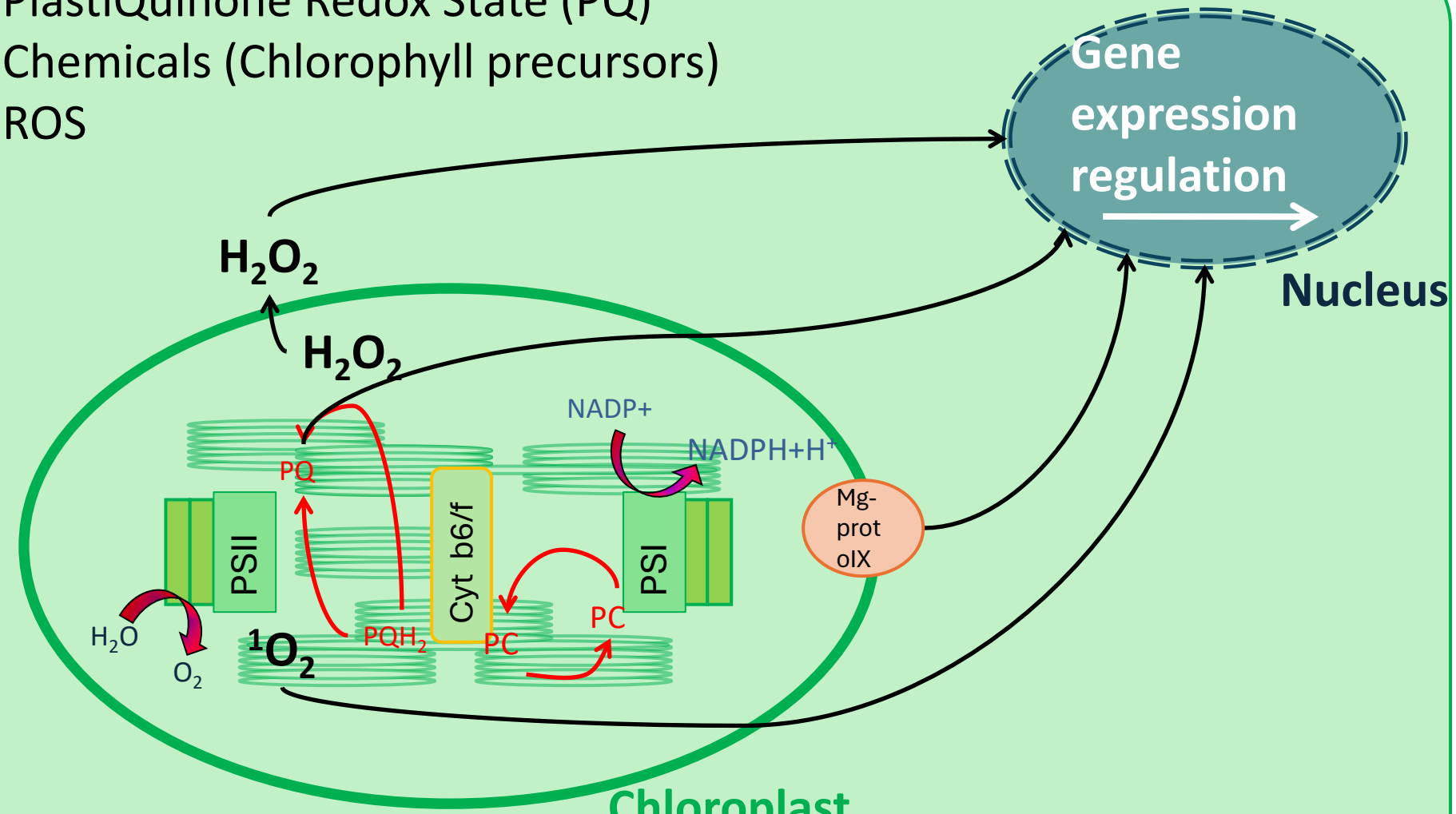

Adapted from Fernandez and Strand COPB 2008

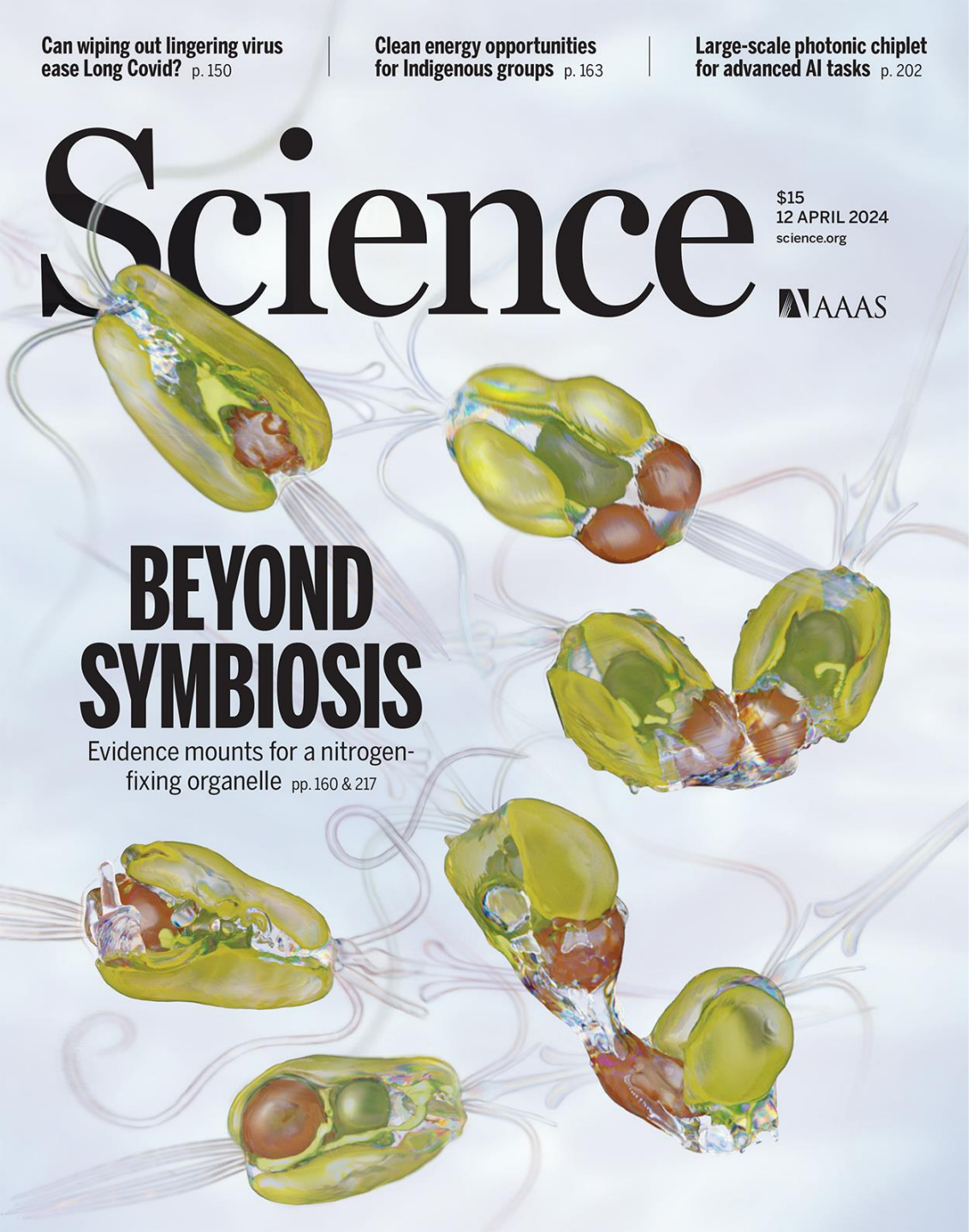

New Discovery: nitroplast

A nitrogen-fixing organelle, or “nitroplast,” has been identified in a marine alga on the basis of intracellular imaging and proteomic evidence. This discovery sheds light on the evolutionary transition from endosymbiont to organelle. The image depicts the cell architecture and synchronized cell division of the alga Braarudosphaera bigelowii with nitroplast UCYN-A (large brown spheres).

Science | AAAS

Evolution and function of the nitroplast

Multiple organelles in eukaryotic cells, including mitochondria, chloroplasts, and nitroplasts, evolved from the integration of endosymbiotic bacteria. In *Braarudosphaera bigelowii*, the chloroplast fixes inorganic carbon to produce glucose, which feeds the respiratory chain in mitochondria that produces adenosine triphosphate (ATP), which in turn fuels nitrogen fixation in the nitroplast. Glucose, ammonia, and ATP generated by the organelles, together with externally incorporated compounds (phosphorous, mineral nutrients, and vitamins), are the building blocks for cell metabolism, resulting in cell growth and division.

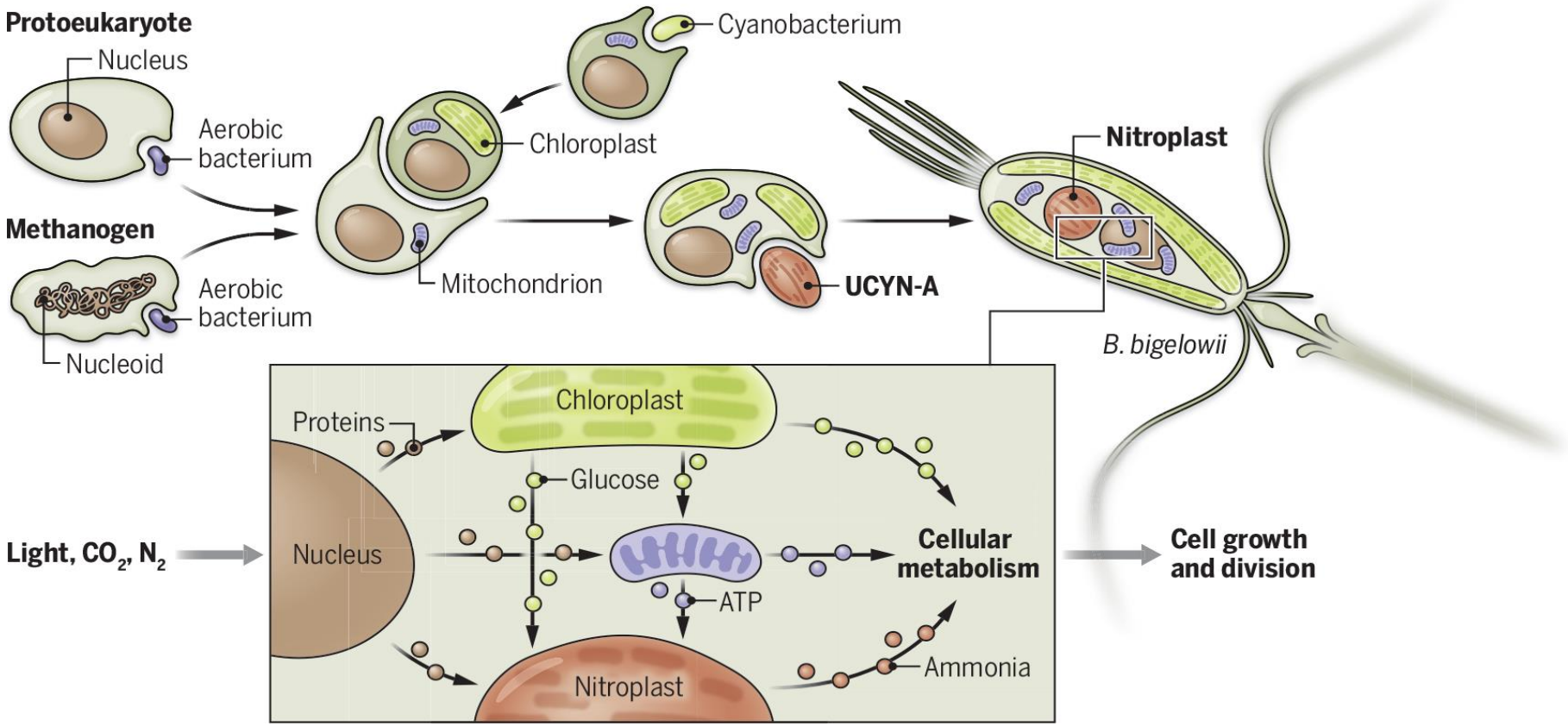

The nitroplast: A nitrogen-fixing organelle, Volume: 384, Issue: 6692, Pages: 160-161, DOI: (10.1126/science.ado8571)

Braarudosphaera bigelowii/UCYN-A lightdark cycle is highly coordinated.

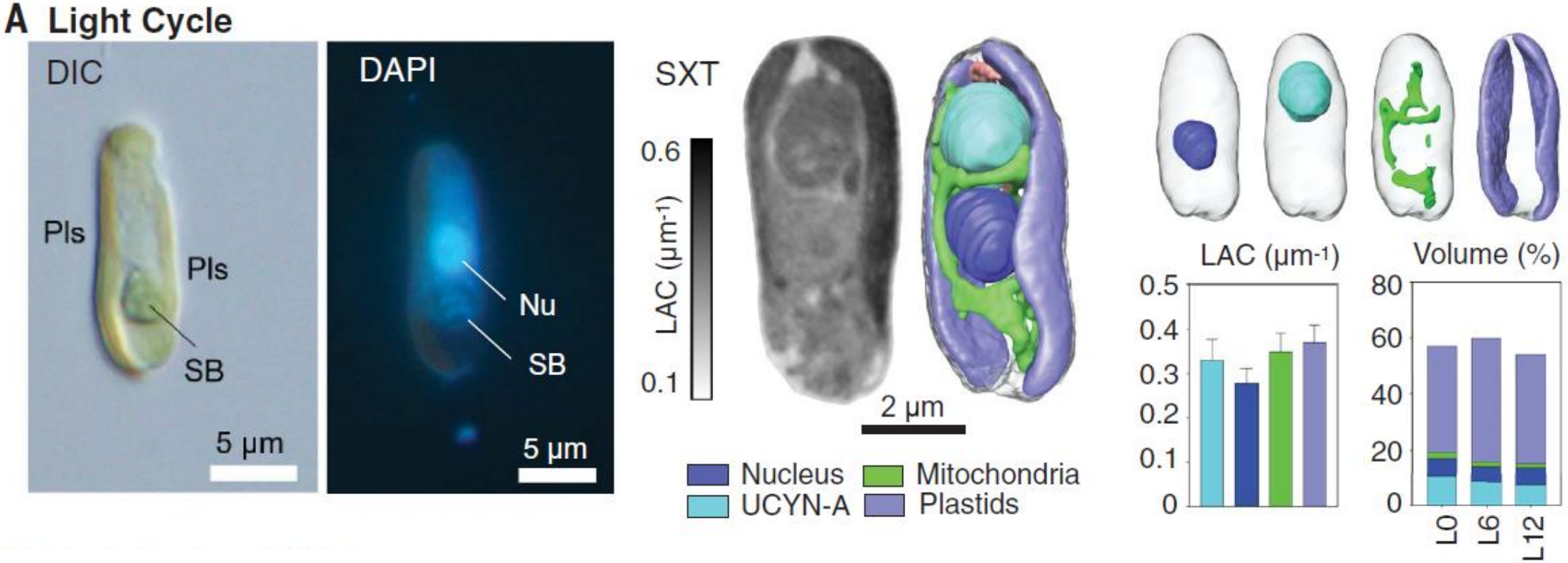

Structural characterization during the light cycle
soft x-ray tomography (SXT)

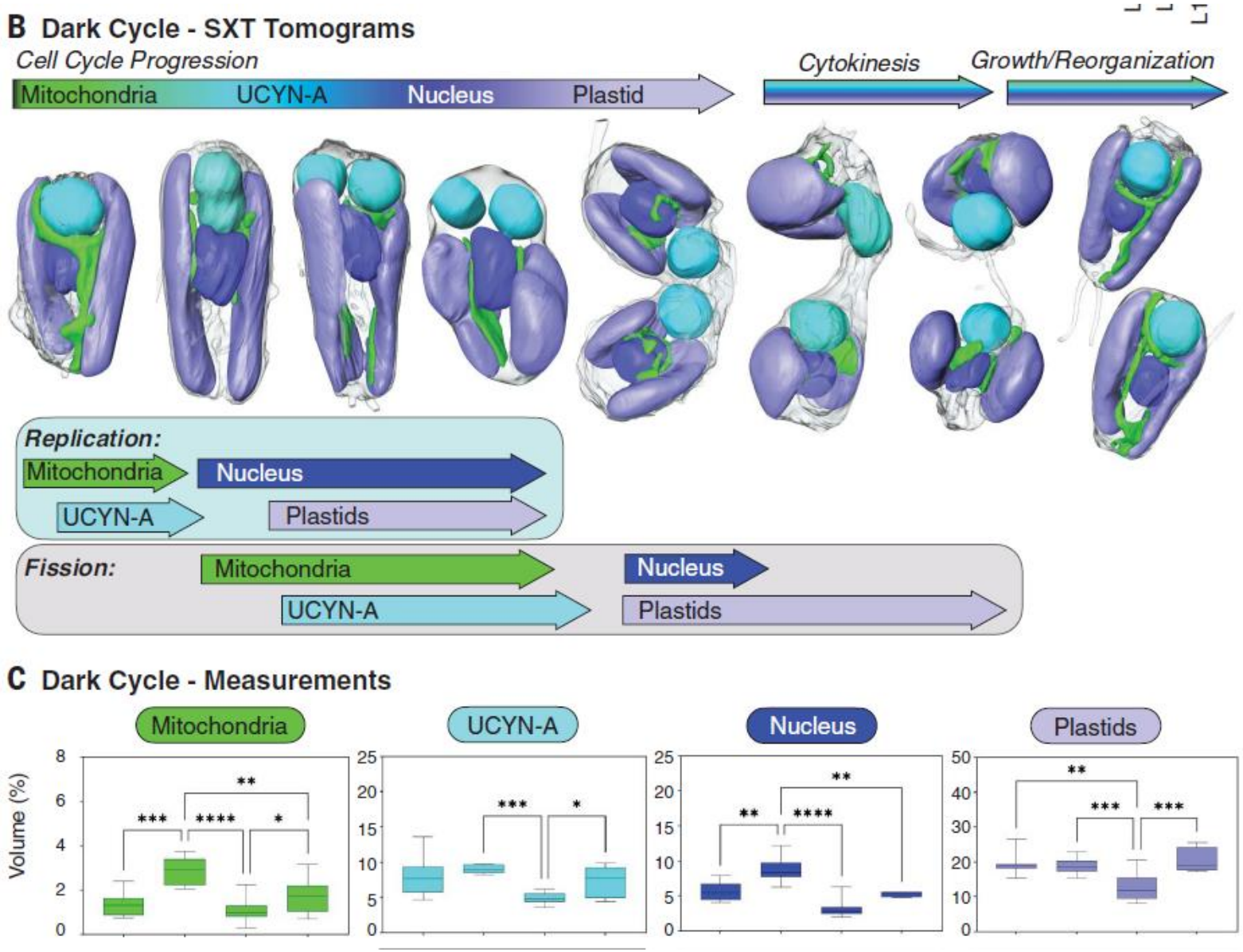
B Dark Cycle - SXT Tomograms
Cell Cycle Progression
Mitochondria
UCYN-A
Nucleus
Plastid
Cytokinesis
Growth/Reorganization
Replication:
Mitochondria
Nucleus
UCYN-A
Plastids
Fission:
Mitochondria
Nucleus
UCYN-A
Plastids
C Dark Cycle - Measurements
Mitochondria
UCYN-A
Nucleus
Plastids
Volume (%)

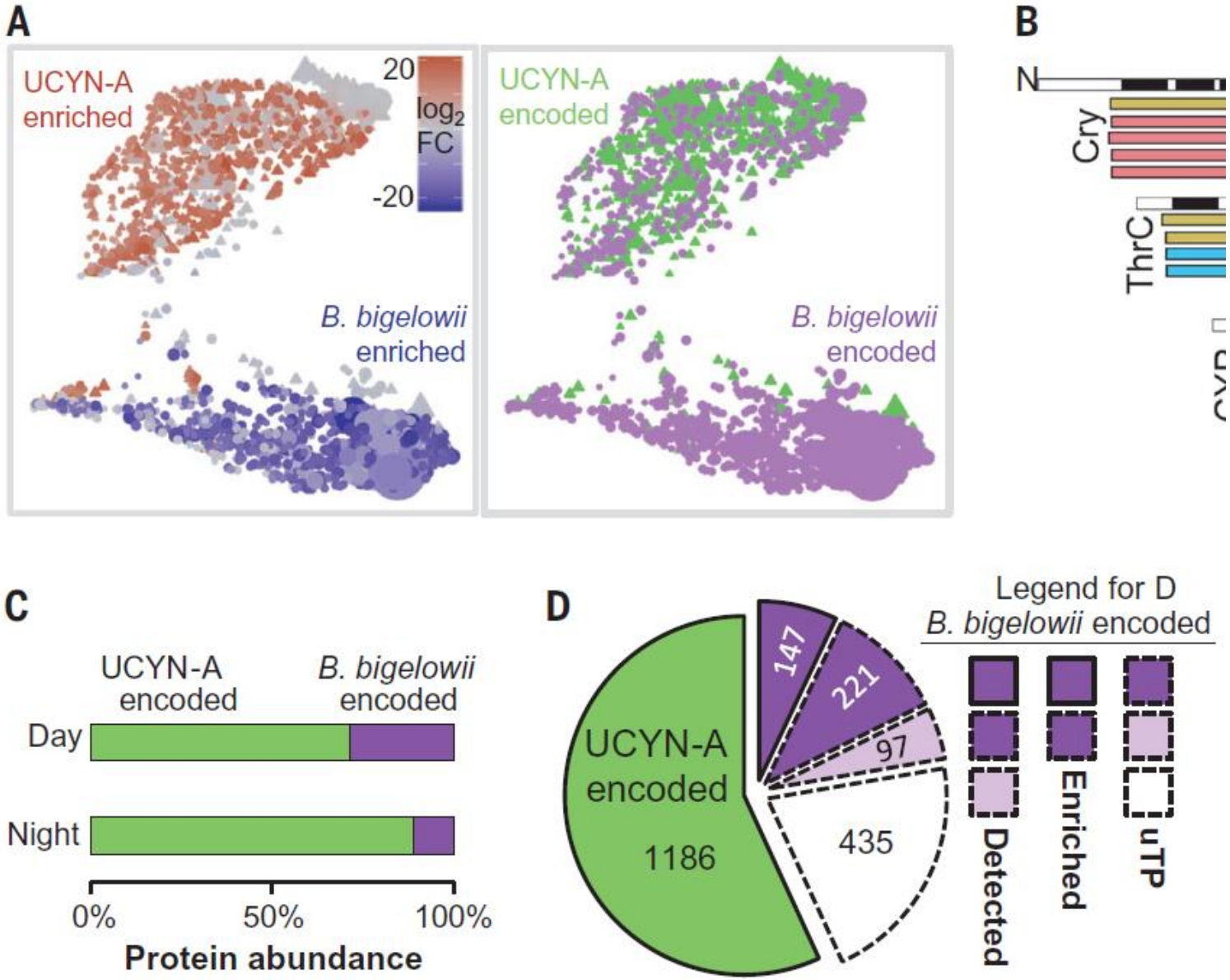
A
UCYN-A
enriched
20
log2
FC
-20
B. bigelowii
enriched
UCYN-A
encoded
B. bigelowii
encoded
B
N
Cry
ThrC
C
UCYN-A
encoded
B. bigelowii
encoded
Day
Night
0%
50%
100%
Protein abundance
D
Legend for D
B. bigelowii encoded
147
221
97
435
UCYN-A
encoded
1186
Detected
Enriched
uTP